Guidelines on dual scanning lidar measurements for wind resource assessments

Rev. 0
5 March 2024

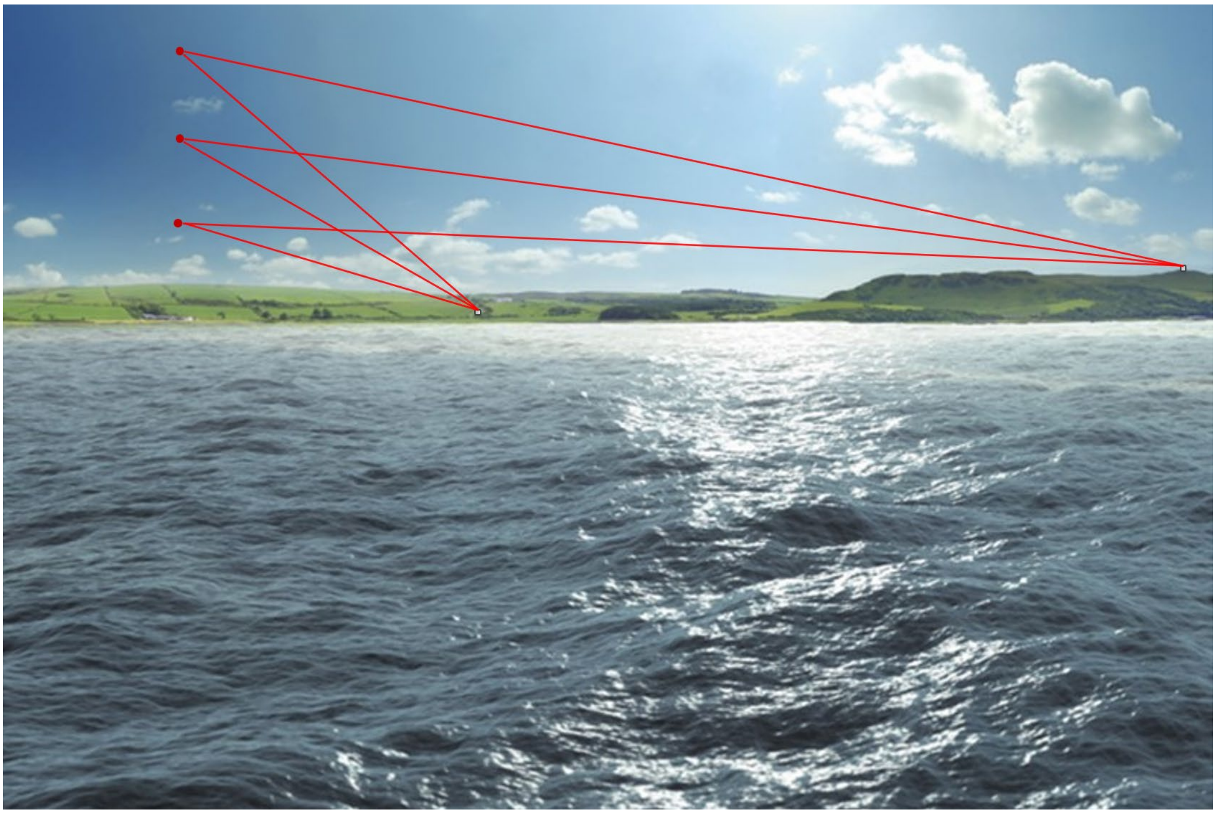

Report Title:	Guidelines on dual scanning lidar measurements for wind resource assessments
Consultant:	DNV Energy Systems Germany GmbH, Brooktorkai 18, 20457 Hamburg, Germany
Organisation unit:	E-NV-M
Date of issue:	5 March 2024
Revision:	0
Confidentiality:	Open

Authors

Dominic Champneys (Vaisala)

Richard Frühmann (DNV)

Robert Menke (DNV)

Darshan Sathiyanarayanan (Vaisala)

Matthias Steger (DNV)

Reviewers

Andrew Black (Vaisala)

Matthieu Boquet (Vaisala)

Reesa Dexter (DNV)

Jens Riechert (EnBW)

Table of contents

List of tables

List of figures

Abbreviations

CNR	carrier to noise ratio – a measure of how strong a signal is compared with the background noise
DSL	dual scanning lidar – a measurement setup using two lidars that scan and operate together to provide wind speed measurements
EDFA	erbium doped fibre amplifier – signal amplifier used in laser technology
GPS	global positioning system
IEA	International Energy Agency
IEC	International Electrotechnical Commission
KPI	key performance indicator – parameters used to assess the performance of a system
Lidar	light detection and ranging
LOS	line-of-sight – along the laser beam
NTP	network transfer protocol
PPI	plan position indicator – scans in which the azimuth is varied continuously while maintaining a constant elevation angle
SMC	specific measurement campaign
UPS	uninterruptable power supply
UTM	universal transverse Mercator – a map projection in which the curved surface of the earth is divided into 60 zones of 6° longitude each, and each zone is approximated to a flat surface
WFR	wind field reconstruction – the process by which individual LOS wind speeds are combined to calculate the corresponding horizon wind speed and direction.

Nomenclature

A_{ϕ}	Amplitude of the sinusoidal elevation angle offset
A_{θ}	Amplitude of the sinusoidal azimuth angle offset
a	slope of the linear regression
b	offset of the linear regression
C_{vLOS}	KPI defining the limits for the mean of the difference in the LOS wind speed between lidar and reference expressed as a percentage of the mean LOS wind speed of the verification campaign
HWS	reconstructed horizontal wind speed
O_{ϕ}	Offset of the of the sinusoidal elevation angle offset
O_{θ}	Offset of the sinusoidal azimuth angle offset
OFF_{vLOS}	KPI defining the limits for the offset of the linear regression of the LOS wind speed (lidar vs. reference)
P_{ϕ}	Phase of the sinusoidal elevation angle offset
P_{θ}	Phase of the sinusoidal azimuth angle offset
R	Range along the LOS, distance from the lidar to the centre of the probe volume
R^2_{vLOS}	KPI defining the limits for the coefficient of determination of the linear regression of the LOS wind speed (lidar vs. reference)
u, v, w	orthogonal vector components of the wind speed
u_{cal}	uncertainty of the calibration of the reference wind speed sensor
$u_{class_{LOS}}$	uncertainty of the classification pertaining to the LOS wind speed
u_{daq}	uncertainty arising from the data acquisition system of the reference
$u_{ext_{\phi}}$	uncertainty of the extrapolation of the measured elevation offsets
$u_{HWS_{WFR}}$	cumulated uncertainty after propagation of intermediate values through the wind field reconstruction
$u_{HWS_{10min}}$	uncertainty associated with each individual 10-minute average HWS
u_{inc}	uncertainty in the measurement height resulting from beam inclination
u_{mast}	uncertainty from reference met mast configuration
u_{move}	uncertainty arising from motion of the lidar
u_{ope}	operational uncertainty – the uncertainty from the device classification of the reference wind speed sensor
u_{pos}	uncertainty due to the mounting of the lidar and the terrain
u_R	uncertainty of the range
u_{ref}	uncertainty of the reference wind speed sensor (as installed)
$u_{ref_{\phi}}$	uncertainty of the elevation reference angle
$u_{rep_{\phi}}$	uncertainty of the repeatability of the elevation angle calibration

$u_{schedule}$	uncertainty arising from the scan schedule
u_{stab_ϕ}	uncertainty of the long-term elevation angle stability
u_{stat}	statistical uncertainty
u_{terr}	uncertainty due to wind speed variations within the measurement volume
u_{veri}	LOS wind speed uncertainty resulting from the verification campaign
u_{vert_pos}	uncertainty due to the height difference between the reference and the LOS range gate
$u_{v_{LOS}}$	total LOS wind speed uncertainty
$u_{WFR_{suit}}$	uncertainty associated with the suitability of the wind field reconstruction
$u_{\Delta\Theta}$	uncertainty in the relative wind direction (wind direction – LOS azimuth)
u_{Θ}	uncertainty of the calibration of the reference wind direction sensor
u_{θ}	uncertainty of the azimuth angle
u_{ϕ}	uncertainty of the elevation angle
v_{HWS}	horizontal wind speed of the reference sensor
v_{LOS}	LOS wind speed – vector component of the wind speed parallel to the laser beam
v_{ref}	reference wind speed (projected onto the LOS)
X_{vLOS}	KPI defining the limits for the slope of the linear regression of the LOS wind speed (lidar vs. reference)
Θ	horizontal wind direction
θ	azimuth of the LOS – angle of rotation about the vertical axis
ϕ	elevation of the LOS – elevation is the angle relative to the horizontal plane

1 INTRODUCTION

Scanning light detection and ranging (lidar) technologies are finding increasing use for wind speed measurements, especially in the field of wind resource assessments for the wind energy industry. Two key advantages of scanning lidars compared to other wind measurement technologies are:

1. They enable multiple measurement locations to be interrogated with a single measurement setup, and
2. Their long-range capability enables measurements at inaccessible locations.

This can help to reduce costs and logistic efforts, for example when measuring wind speed over the sea from locations on the coast, or if interrogating multiple locations in a large planning area with limited access and infrastructure.

The aim of this document is to provide guidance in the absence of an existing standard. By sharing practical insights and best practices in campaign planning and execution, uncertainty assessment, and documentation it may facilitate the decision-making process and make the technology more accessible to potential users.

Although other applications and modes of operation are possible, this paper is limited to the application of scanning lidars in a so-called dual scanning lidar (DSL, or dual Doppler lidar) configuration for wind resource assessment campaigns in reasonably uniform flows. This means that only the measurements of horizontal wind speed (HWS) and direction are considered, and turbulence measurements are not discussed. The dual scanning lidar configuration has been chosen because it is a popular use case with a well-defined scope and a limited number of adjustable variables.

The document begins with an outline of a typical project workflow. Details of the individual steps are referenced to the respective sections, thereby serving as a guide to the user who may be interested in only a particular aspect of the project lifecycle. This is followed by an introduction to the underlying theory, typical use cases, methods, and relevant parameters to provide a common basis in terms of the terminology typically used when talking about scanning lidars and their application. It continues with targeted sections that describe planning a campaign, verifying the devices, installing and commissioning the equipment, and operating a campaign. The final section considers the estimation of measurement uncertainties both pre- and post-campaign. Each section ends with recommendations for reporting and documentation.

It is acknowledged that other documents with similar scopes to this work are available, for example [1] and [2]. This document is not intended to replace those documents but rather to complement them. There is ongoing work to produce further standardisation, notably the International Energy Agency (IEA) task 52 working group, which aims to write a recommended practice for the use of scanning lidars in offshore measurements, and the upcoming International Electrotechnical Commission (IEC) standard 61400-50-5, which will be a technical specification for wind measurements using scanning lidars within the domain of wind energy generation systems. Again, this document aims to exist in conjunction with these standards and to inform their development where the scopes overlap.

2 TYPICAL CAMPAIGN WORKFLOW

The workflow below outlines the different phases of a typical DSL campaign for wind resource assessment. The individual steps are presented in typical chronological order. This document does not follow the campaign workflow structure directly. Reference is made to the relevant sections of this document where further information relating to the individual tasks can be found.

I. **Campaign planning *(see Section 4)***

a. Define the general area of desired measurement points.
b. Identify possible installation locations, landowners, and permitting agencies.
c. Compute resulting scan geometries and estimate uncertainties and ranges.
d. Select the best installation locations; if none are found to be suitable, repeat previous steps.
e. Select a suitable lidar able to fulfil range and availability requirements.
f. Identify suitable method and references for pointing accuracy tests.

II. **Lidar pre-verification *(see Section 5)***

a. Choose verification approach.
b. Install and commission lidars at verification site.
c. Monitor the measurement system.
d. Calculate uncertainties and report the results.

III. **Installation and commissioning *(see Section 6.1)***

a. Install lidar as per manufacturer guidelines.
b. Perform pointing accuracy tests and, if applicable, on-site wind speed verification.
c. Setup the network connection, time synchronisation, and scan parameters according to plan.
d. Setup data transfer and monitoring processes.
e. Document commissioning activities including alignment offsets and reference targets.

IV. **Operation and monitoring of the specific measurement campaign *(see Section 6.2 and Section 6.3)***

a. Monitor system performance regularly, including system alignment checks.
b. Register significant events (e.g., changes in setup, maintenance, etc.) in a campaign log.
c. If changes to system position are detected during the campaign, adjust the scan pattern as necessary.
d. Conduct repair or maintenance work if necessary.

V. **Data processing *(see Section 6.4)***

a. Filter data set to remove invalid measurements.
b. Reconstruct the wind speed and directions from line-of-sight (LOS) data.
c. Calculate availability and wind speed and direction statistics.
d. Report the results.

VI. **Uncertainty evaluation *(see Section 7)***

a. Calculate the uncertainty of intermediate values that are used in the wind field reconstruction (WFR).
b. Calculate the uncertainty of reconstructed wind parameters.
c. Document the calculations and report the results.

VII. **Decommissioning and post-campaign verification *(see Section 5)***

a. Decommission and retrieve equipment from campaign site.
b. If required, perform a post-campaign verification using the same method as the pre-campaign verification.

The following flowchart indicates a typical timeline of a dual scanning lidar campaign for wind resource assessment including the different project phases described above.

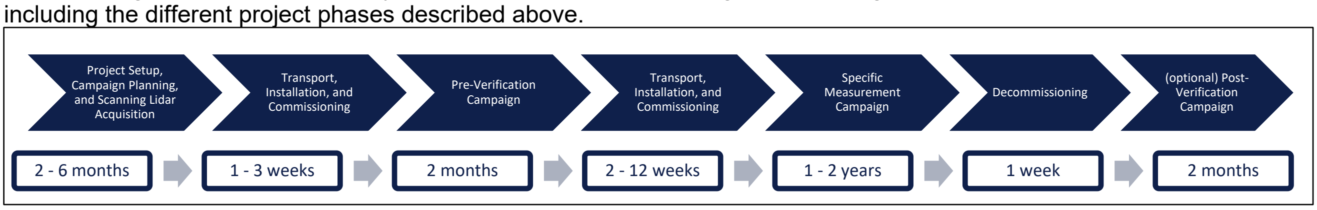

Figure 2-1 Typical scanning lidar campaign timeline

3 DUAL SCANNING LIDAR PRINCIPLE

3.1 Overview

This section aims to define a common basis for understanding the lidar technology and terminology to be used in the rest of the document. The underlying mathematics and theory will be presented, and thereby also a set of vocabulary that will be used in this document in reference to scanning lidar measurements. This section is intended to explain the effects of various parameters in a relative sense, without necessarily giving a specific recommendation or optimum value. More specific guidance is given in Section 4, citing the effects described here.

Lidars in this document are devices that use the Doppler effect on backscattered lasers to measure wind speed. Scanning lidar refers to a type of lidar device with the ability to point the laser in any direction (typically limited approximately to the hemisphere above the device) and in general provides measurement to much greater distances than vertical or turbine-mounted lidars.

Because lidars are only able to measure the wind speed vector component in line with the laser beam (the LOS wind speed), the horizontal wind speed and direction needs to be reconstructed from multiple beams with different orientations. The reconstruction of the wind vector using one or more scanning lidars can be done using a variety of different methods, geometries, and modes of operation, each with advantages, drawbacks, and special considerations.

The DSL configuration refers to a setup in which two scanning lidars measure the same point in space at different beam angles, allowing the wind vector to be reconstructed (assuming a statistically negligible vertical wind speed component) at a well-defined location. The assumption of the purely horizontal flow limits this application with only two scanning lidars to flat terrain, as typically found offshore or in simple terrain. It is acknowledged that single scanning lidar reconstruction can also provide valid wind vector measurements; however, it is not in the remit of this document to give guidelines for single scanning lidar reconstruction. Further explanation and a comparison between single and dual scanning lidar measurements is presented in [3].

This section describes how two individual LOS wind speeds can be combined into a horizontal wind vector and how the parameters of the scan, beam geometries, and operational considerations can affect this calculation.

3.2 Wind field reconstruction

The LOS wind speed measured by a single scanning lidar can be expressed in terms of the orthogonal wind vector components, *u*, *v*, and *w* as in Equation 1.

$$-v_{LOS} = u.sin\theta.\cos\phi + \mathrm{v}.\cos\theta.\cos\phi + \mathrm{w}.\sin\phi \quad (1)$$

where θ is the azimuth angle and ϕ is the elevation angle, *u* and *v* are the horizontal vector components, *w* is the vertical vector component, and v_{LOS} is defined as negative for wind coming towards the lidar. The orthogonal axes are defined in meteorological convention, with *v* orientated north, and angle θ increasing in the clockwise direction and indicating the direction from which the wind is blowing (i.e., our wind vector points in the direction opposite to the motion of the air particles), as shown in Figure 3-1.

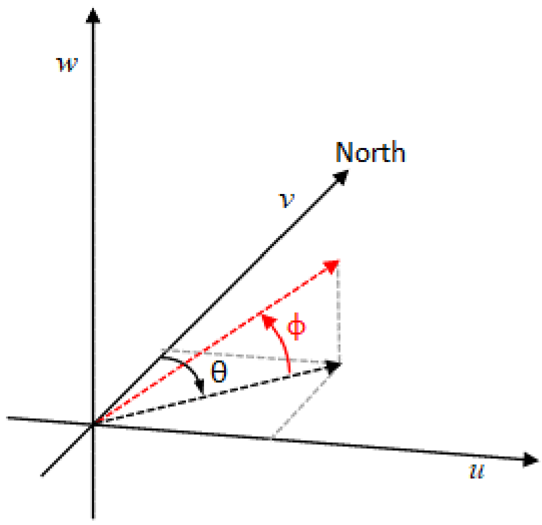

Figure 3-1 Sign convention for orthogonal wind vector system

This can then be extended to a dual scanning lidar setup as in Equation 2a using the projection matrix ***M***, defined in Equation 2b.

$$\begin{bmatrix} -v_{LOS1} \\ -v_{LOS2} \end{bmatrix} = \boldsymbol{M}.\begin{bmatrix} u \\ v \\ w \end{bmatrix} \quad (2a)$$

$$\boldsymbol{M} = \begin{bmatrix} sin\theta_1 cos\phi_1 & cos\theta_1 cos\phi_1 & sin\phi_1 \\ sin\theta_2 cos\phi_2 & cos\theta_2 cos\phi_2 & sin\phi_2 \end{bmatrix} \quad (2b)$$

The vertical wind component can be separated from the horizontals to give Equation 3a, using a reduced projection matrix that is defined in Equation 3b.

$$\begin{bmatrix} -v_{LOS1} \\ -v_{LOS2} \end{bmatrix} = \boldsymbol{M}_{reduced}.\begin{bmatrix} u \\ v \end{bmatrix} + \begin{bmatrix} sin\phi_1 \\ sin\phi_2 \end{bmatrix}.w \quad (3a)$$

$$M_{reduced} = \begin{bmatrix} sin\theta_1 cos\phi_1 & cos\theta_1 cos\phi_1 \\ sin\theta_2 cos\phi_2 & cos\theta_2 cos\phi_2 \end{bmatrix} \quad (3b)$$

As the reduced matrix is no longer underdetermined, it can be inverted. This allows for Equation 3a to be solved for the wind vector components by neglecting the term involving the vertical wind speed, shown in Equation 4. It can be observed that the assumption made in this step has a negligible impact on *u* and *v* when either the vertical wind speed component is close to zero (often the case offshore or in simple terrain), or when the elevation angle is close to zero (often the case when using long-range scanning lidars).

$$\begin{bmatrix} u \\ v \end{bmatrix} = \boldsymbol{M}^{-1}_{reduced}.\begin{bmatrix} -v_{LOS1} \\ -v_{LOS2} \end{bmatrix} \quad (4)$$

The expanded equations for *u* and *v* are shown in Equations 5a and 5b and those for the horizontal wind speed and direction in Equations 6a and 6b. Note that the exact Equations 5 and 6 used to calculate *u*, *v,* and the wind direction will differ based on the convention used for *u*, *v*, and v_{LOS}.

$$u = \frac{v_{LOS2} cos\theta_1 cos\phi_1 - v_{LOS1} cos\theta_2 cos\phi_2}{cos\phi_1 cos\phi_2 sin(\theta_1 - \theta_2)} \quad (5a)$$

$$v = \frac{v_{LOS1} sin\theta_2 cos\phi_2 - v_{LOS2} sin\theta_1 cos\phi_1}{cos\phi_1 \, cos\,\phi_2 sin(\theta_1 - \theta_2)} \quad (5b)$$

$$HWS = \sqrt{u^2 + v^2} \quad (6a)$$

$$\Theta = atan2(u, v) \quad (6b)$$

3.3 Mode of operation

3.3.1 Point-intersect versus scanned area

The most common approach used for DSL measurements is the so-called "point-intersect" approach where the two scanning lidars are coordinated so that their beams intersect at one point, at which the horizontal wind vector is derived. The only spatial averaging done in this mode is that within the probe volume of the lidars, largely along the beam, and so the sensitivity to atmospheric inhomogeneity is minimal. The downside to this method is that the wind speed is only reconstructed at the point of intersection, rather than providing data across an area or volume. However, over a 10-minute period it is common to see the lidars configured to switch between multiple intersection points to give data at several locations and heights.

A second approach combines plan position indicator (PPI) scans from both lidars to reconstruct the data over the area covered by both sweeps. This implies that the reconstruction is done with LOS measurements that are not both co-located and synchronised and therefore makes assumptions regarding the homogeneity and time invariance of the wind field when reconstructing the wind field. This introduces a degree of uncertainty regarding the effect of atmospheric inhomogeneity on the calculated wind speed, even in relatively stable conditions. The advantage is that this method will yield a spatially distributed wind speed estimate, representative of a larger area or volume. The LOS wind speeds at individual range gates can further be interrogated to provide an estimate on the variation within the wind field.

3.3.2 Synchronisation

When measuring at more than one location, the time taken to complete one full scanning trajectory is not always the same between the two lidars. Without an active effort to synchronise the scan patterns, this leads to the lidars measuring at each of the set locations at different times. The consequence is that the measurement uncertainty increases. The ability to actively synchronise multiple lidars depends on the make and model, as well as on the existing communications links at the installation sites. At many locations, active synchronisation can be difficult. In this case, it is recommended that an effort be made to ensure the best possible synchronisation, for example: through careful design of the scan patterns, or through regular restarts of the scan patterns according to a common time reference e.g., a global positioning system (GPS) clock or a network transfer protocol (NTP) server. The maximum and mean deviations between the two lidars can be assessed during the campaign, so that this effect can be considered in the uncertainty calculation. Reference [4] provides further discussion on the effect of synchronisation between multi-scanning lidar measurements.

3.3.3 Number of measurement locations and measurement frequency

Having multiple measurement locations is a trade-off between temporal resolution at any single position in space versus increased information about the spatial variation in wind speed. Increased spatial coverage or resolution reduces the uncertainty associated with extrapolating a single wind speed measurement location over an area. While measuring more locations over a certain period decreases the frequency at which each position is measured, the measurement frequency has a limited effect on the precision of the average wind speed measurements.

3.4 Beam geometry

3.4.1 Beam intersection angle

The HWS is composed of two perpendicular components and so, in theory, to capture it fully with two one-dimensional LOS wind speed measurements, the beam azimuth angles should also be perpendicular. In practice we can use geometry to project the measurements of any two different beam angles onto the *u* and *v* components. However, if the two beams are close to parallel, the uncertainty of the WFR becomes very large in the wind sector that is perpendicular to the two beams as the projection of the HWS onto the beams is very small and any uncertainty on these LOS wind speeds is greatly magnified [5] [6].

3.4.2 Elevation angle

In the WFR equations given in Section 3.2, the projection of the vertical wind speed was assumed to be negligible. The projection of the vertical wind speed onto the LOS wind speed is non-zero if two conditions are met: a non-zero vertical wind speed and a non-zero elevation angle of the beam. In the real atmosphere there is always some, even if very little, vertical wind speed component and the larger the elevation of the beam the more it will be projected onto the LOS wind speed. A lower elevation angle of the beam therefore gives a lower sensitivity to vertical wind speed in the atmosphere.

3.4.3 Range

The primary consideration of measurement range is that of data availability – at longer ranges less light is successfully backscattered to the lidar and data availability is therefore reduced. The range at which a suitable data availability can be achieved depends on the model of scanning lidar, the measurement configuration, and the atmospheric conditions.

A secondary effect of the range is that a longer range will mean more vertical displacement with a given offset of elevation angle. An uncertainty in the elevation angle translates to an uncertainty in the measurement height, which in turn translates to an uncertainty on the wind speed measurement due to the shear profile – a longer measurement range accentuates this effect.

3.5 Scan parameters

3.5.1 Range gate length

The range gate length is the probe length of the lidar. When choosing a range gate length, two effects should be weighed against each other. Increasing the range gate length results in an increase in spatial averaging of the measurement and thereby an attenuation of velocity variations. On the other hand, a longer range gate provides more backscattered photons that are accumulated per sample. Therefore, by increasing the range gate length, data availability at long ranges can be improved. Since the attenuation of velocity variations has a small effect on the mean wind speed in simple atmospheric flows, data availability is often the dominant consideration when choosing a range gate length for wind speed and direction measurements.

3.5.2 Accumulation time

The accumulation time is the amount of time over which return spectra from successive pulses are accumulated and averaged for a single LOS wind speed measurement. Increasing the accumulation time increases the temporal averaging of each sample and decreases the frequency of the measurement. Increasing the number of averaged spectra makes the signal clearer above the noise and therefore a longer accumulation time can improve the data availability.

3.5.3 Dwell time

The dwell time refers to the amount of time during which the scan head remains in one position before moving to the next measurement location. The minimum dwell time is the time taken to acquire a single sample (i.e., the accumulation time). Increasing the dwell time reduces the proportion of time taken up by the scanner moving between measurement positions and so implies a modest increase in the number of samples that can be collected over 10 minutes. However, this leads to uneven sampling (i.e., several samples are taken in close succession with a subsequent longer gap until the scan cycle returns to the same position), which distorts statistics. Current experience suggests that using the minimum dwell time gives the most representative 10-minute statistics [7].

3.6 Note on turbulence

Although dual scanning lidars have been identified as a suitable instrument to measure turbulence intensity (see [8], [9]), it is beyond the scope of this version of this paper to provide guidance on turbulence intensity measurements. It should be noted that some of the guidance provided herein would change if it were to consider turbulence intensity measurements, notably those concerning measurement frequency, range gate length, and accumulation time.

4 CAMPAIGN PLANNING AND PREPARATION

4.1 Overview

This section presents a recommended procedure that can be followed when designing a measurement strategy using DSLs to conduct a wind resource assessment in simple (flat) terrain as typically found offshore. These recommendations are based on scientific reasoning outlined in Section 3 and practical experience. However, given that the requirements of individual cases differ (and it is often possible to balance the non-optimum value of one parameter with a close-to-optimum value of another) they should be seen as guidelines rather than hard rules.

The design stage of a DSL campaign should consider the needs of the project and how the setup can be made to best address them. The design should be done in an iterative manner, with one consideration (e.g., desired measurement locations) informing another (e.g., beam geometry), which can inform the original consideration (e.g., changing measurement locations to improve beam geometry). As many crucial aspects of a DSL campaign can be assessed at this stage, the feasibility of the project can also be assessed before any further investment is made.

4.2 Campaign design

4.2.1 Measurement locations

This document assumes that the lidars operate in a point-intersect mode as described in Section 3.3.1. In this mode of operation, the lidars move in a synchronised manner to defined measurement positions and remain there for a fixed period of time before moving to the next position. This means that the sampling interval at each measurement location depends on the number of points to be measured, and the time taken for the scanner to move between points.

The number and location of measurement points will depend on the project requirements. Where there is interest in obtaining measurements spread over a large area and/or multiple elevations, a trade-off needs to be made between spatial and temporal resolution.

With a typical configuration, it is common to measure 3-9 different measurement points, for example arranged in three "virtual met-mast" vertical profiles each with three measurement heights. Because the uncertainty is linked to the measurement frequency and not the number of points, the maximum number of measurement points for a given campaign will depend on the time to travel between each point and therefore the layout of the campaign and the rotation speed of the scanning head. From experience, a minimum of two measurements per minute at each location can still provide representative 10-minute mean wind speeds—this would limit the maximum number of possible measurement points to approximately 15–20. However, it is not always desirable to use the maximum number of measurement points, therefore pushing the limits of the measurement uncertainty, if it does not bring increased value to the project. In certain situations if may be desirable to measure even more points at the expense of the measurement uncertainty, although in this case it is advised that the measurement frequency be replicated during the verification campaign.

When selecting the measurement points, it is advised to consider that the two intersecting beams should have a suitable beam geometry between them (see Section 4.2.3) at all measurement locations.

4.2.2 Coordinate system

Care should be taken when choosing the coordinate system to use when calculating beam geometry. It is recommended that all calculations be made within the same coordinate system.

In most applications, scanning lidar campaigns cover ranges of 10 km or less. At such distances, an orthogonal (or cartesian) coordinate system such as the universal transverse Mercator (UTM) projection is appropriate. If the area of interest is close to the edge of a UTM zone, especially at higher latitudes near the earth's polar regions, significant distortions may occur in the conversion between spherical and orthogonal coordinate systems (e.g., between longitude/latitude and UTM locations). Care should therefore be taken when using UTM coordinates in conjunction with hard targets for determining the scanner orientation and the beam geometry to avoid errors in defining the scan geometry.

4.2.3 Beam geometry

Beam geometry in this document considers the relative pointing angles of the lidars with respect to each other. The beam geometry forms a triangle with the two lidars and the measurement point at the corners, as shown schematically in Figure 4-1. The beam intersection angle has a critical influence on the measurement uncertainty, as described in Section 3.4.1. Unlike profiling lidars, the measurement uncertainty varies with both the beam geometry and the wind direction. This should therefore be given careful consideration and be clearly documented during the campaign design phase.

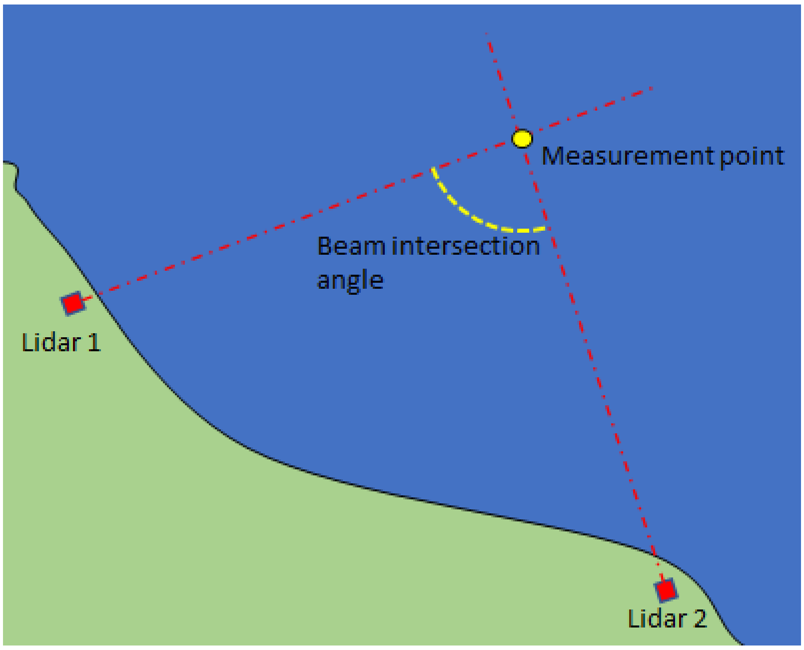

Figure 4-1 Schematic of typical DSL setup showing the two lidars, the measurement point, and the beam intersection angle

The elevation angles used in DSL campaigns are typically less than 5°. At these angles, the vertical component of the wind speed has a negligible effect on the measurement. When defining multiple measurement heights or positions at varying distance, the possible influence of the vertical wind speed component on the measurement should be documented, as this may vary for each measurement location. Besides other components, when calculating elevation angles a correction should be made to the measurement height to account for the curvature of the earth.

The final component of beam geometry is the range. This will mostly impact data availability and needs to be considered when choosing the appropriate lidar, integration time, and range gate length. In general, the availability will decrease with increasing range. For wind resource assessments, a typical rule of thumb is to aim for a post-processed data availability of 80% to 90% [10], [11]. If the main area of interest is situated at a range where it will be difficult to achieve suitable data availability, adding an additional measurement point at shorter range for the purpose of gap filling could be considered. Since the site-specific atmospheric conditions will determine the range performance of any given lidar, it is advised that these be given due consideration during the campaign planning phase, for example through a simulation tool or comparison to other campaigns with similar atmospheric conditions.

4.2.4 Uncertainty assessment

Even in the preliminary design of the layout of a DSL campaign, considerations should be made regarding the effect of the beam geometry on the final measurement uncertainty. To avoid calculations over a potentially infinite number of beam geometries, the search area for potential installation sites of each lidar, can be identified by considering the following guidelines:

- A beam intersection angle of 30-150° [5], [12]
- An elevation angle of each beam lower than 5°

Once a finite number of potential installation sites within these areas have been identified, a calculation of uncertainty (the process for which is detailed in Section 7) can be done, whilst making some assumptions about wind conditions on site, to find the combination of locations with the lowest uncertainty relative to the desired measurement positions. It is advised that the final selection of installation locations be made based not only on which give the lowest uncertainty but also considering other aspects of the sites, such as those listed in Section 4.4; especially when the difference in uncertainty between two options is small.

Note that breaching the guideline limits listed above does not necessarily imply that a candidate layout is unfeasible. In this case it is recommended to follow the full process of uncertainty calculation detailed in Section 7 to check that the final uncertainty is acceptable.

4.3 Lidar requirements

4.3.1 Overview

This section provides a list of recommended specifications to which any model of scanning lidar chosen for use in a DSL campaign should conform. A suitable lidar system preferably has a track record of operation under different conditions over which it can be assessed if the system can meet these recommendations or not. If this is not available, it is advised that tests be performed and documented that prove the ability to meet the recommended performance.

4.3.2 Requirements

Most fundamentally, the lidar needs to be able to accurately measure the LOS wind speed. How to assess the accuracy or uncertainty is described in Section 7.

The scanner needs to have a sufficient pointing accuracy for the specific scan geometry. The elevation pointing accuracy is most critical since the wind speed varies most strongly with height. To determine the pointing accuracy requirements for the specific measurement campaign, the following parameters should be considered:

- Measurement heights
- Measurement range
- Mean wind speed
- Wind shear
- Wind speed uncertainty requirement

For details of methods to determine the pointing accuracy, refer to Section 5.3.

Furthermore, it is recommended that the scanner is equipped with inclinometers (internal or external) that enable changes in the orientation of the device that may occur during the campaign to be detected. Depending on the application, the required sampling rate of these sensors will vary; for example: a lidar positioned on the transition piece of an offshore wind turbine will experience changes in inclination at a much higher rate and therefore require a higher sampling rate compared to a lidar installed on a concrete plinth at a coastal site. In the offshore case, a sampling rate greater than or equal to the LOS sampling rate is recommended.

The chosen scanning lidar systems should have the connectivity to allow for:

- Synchronisation between the two systems with the maximum time difference not exceeding 2 seconds.
- Synchronisation of the two systems to the same reference time (for example using GPS time or an NTP server).
- Routine monitoring of the system and its sub-components so that any malfunction can be detected as quickly as possible.
- The reliable transfer of measured data from the system without losing data.
- Traceability of system operation and data, with historical data on the system health and metadata describing under which configuration and conditions the data were recorded.

Given that a failure of one scanning lidar means the unavailability of the whole DSL setup for measurements, the chosen system should exhibit high reliability with preferably an assessable track record of good system availability in different operational conditions. The ability to conduct maintenance or repairs on site for simple problems can help minimise measurement downtime in the event of a system failure. To accommodate cases where on-site repairs are not possible, having a spare lidar available on short notice to be able to replace the malfunctioning scanning lidar whilst it is repaired (or having a redundant measurement setup) can be advisable for remote or difficult to access sites. Maintenance and repair strategy is discussed further in Section 6.3.

4.4 Additional measurement equipment

Additional measurement equipment can add benefit to a campaign including but not limited to:

- Wind measurement equipment (ground based or floating lidars, met masts) which can potentially be used for gap filling, in-situ campaign and post verification, TI correction, etc.
- Measurement equipment for environmental parameters like temperature, humidity, pressure, precipitation, atmospheric stability, etc.
- Equipment supporting the monitoring of the campaign like web cams, visibility sensors, inclinometers, etc.

4.5 Site constraints

For a site to be suitable for the installation of the scanning lidars, the following practical requirements are suggested:

- Ability to obtain the proper legal permission for installation and operation of the lidars
- Safe and accessible to personnel for installation and maintenance
- Security to prevent ingress from unauthorised persons or animals
- Clear LOS to all target measurement locations, free from permanent or transient obstructions
- Sufficient power supply
- Possibility to carry out a pointing accuracy calibration, either through LOS to hard targets, sufficient LOS to the sea surface, or another suitable method

There are several additional considerations which, although not essential, are advised to be present at the installation sites. These are listed below along with suggested alternatives:

- Reliable communication link for synchronisation, data extraction, and monitoring
  - Otherwise, it is advised that an alternative method to maintain synchronisation, extract the data, and monitor the performance and condition of the lidar should be implemented.
- Hard and immobile surface, preferably made of concrete, upon which the lidar can be placed to maintain pointing accuracy
  - If not available, for example when the lidar is placed on a platform with the possibility to move (for example, the transition piece of an offshore wind turbine) it is advised that a method of dynamic pointing accuracy correction is applied.
- Power supply of sufficient stability
  - In the case that the power supply is judged to have significant instabilities, it is advised that an uninterruptible power supply (UPS) be installed to mitigate the effect of power cuts on the continuity of the measurements.

5 VERIFICATION

5.1 Overview

In the field of wind resource assessment, accurate and reliable measurements are paramount to ensure the success of any campaign. As such, it is advised to perform thorough verification of lidars prior to every campaign. Moreover, if there is any source of doubt in the validity of the measurements that arises during the campaign (see Section 5.6), it is advised to perform a post-campaign verification to ensure that the performance of the lidars have not changed during the period of the specific measurement campaign. This section will delve into the importance of lidar verification and highlight two key points: the verification of pointing accuracy and the comparison of lidar-derived wind speeds to reference measurements. By implementing these verification procedures, we can enhance the credibility and quality of the wind resource assessment.

- Pointing accuracy test: One aspect of lidar verification involves assessing the pointing accuracy of the devices. Pointing accuracy refers to the ability of the lidar system to accurately direct the laser toward configured locations.
- Wind speed accuracy test: Verification of the LOS wind speed (for use in so-called “white box” verification of reconstructed parameters) and the verification of reconstructed HWS (so-called “black box” verification).

The aim of the verification is to verify and document that the lidar is functioning correctly and to quantify the uncertainties associated with the wind speed measurement. The upcoming sections describe the methodologies and best practices involved in conducting scanning lidar verifications.

5.2 Requirements to the verification site

To ensure accurate and reliable verification of lidar systems, it is recommended to meet certain requirements at the chosen verification site. These requirements encompass the availability of a reference instrument, appropriate geometry alignment, and a suitable lidar installation location.

- Reference instrument: The reference instrument should meet the following criteria:
    - Height: The measurement should be taken at least 60 m above the ground.
    - Terrain: The terrain surrounding the reference measurement should comply as nearly as possible with the IEC 61400-50-3 [13] simple terrain definition.
    - Calibration and installation: If the reference instrument is an anemometer, it should be calibrated and the installation should be compliant with the guidelines set forth in IEC 61400-50-1 [14]. Otherwise, an appropriate calibration should be carried out and documented in line with the relevant standards.
    - Wind direction measurement: The reference instrument should also feature wind direction measurement capabilities.
- Geometry: The geometry of the verification setup plays a crucial role in obtaining meaningful and representative results. Consider the following factors:
    - Lidar alignment: The lidar systems should be installed in a sector aligned with the prevailing wind direction. This alignment allows the lidars to effectively capture wind data and fill the required bins for LOS wind speed verification within a reasonable time frame.
    - Elevation angle: The elevation angle between the lidar systems and the reference mast should be kept below 5°.

- Lidar installation location: The requirements for the installation location for the verification are the same as those for the campaign: accessibility, power supply, LOS to the reference measurement, and a stable foundation. For further details refer to the guidelines in Section 4.4.
- Measurement sector: The reference and lidar measurements should not be affected by the wake of a neighbouring turbine or an obstacle. The significance of a turbine or an obstacle and the sector to be excluded can be determined following the equations given in IEC 61400-12-1:2017, Annex A [15]. The sector caused from a significant turbine or obstacle can still be used for the verification if it can be shown that it does not have an effect on the correlation of LOS and reference wind speeds.

5.3 Scanner head pointing accuracy

5.3.1 Overview

In contrast to lidars with fixed beam geometries, scanning lidars can typically point in any direction within a hemisphere. The accuracy and repeatability with which the scanner head can target any given position should therefore be assessed as part of the verification campaign. It should be noted that separate tests employing different methods might be applied for verifying the pointing accuracy in the azimuth and elevation directions.

The factors influencing pointing accuracy can be split into three categories:

- System specific factors that are determined during the verification and are assumed to be constant for the subsequent specific measurement campaign (SMC).
- Installation specific factors that are assessed each time the lidar is installed at a new location.
- Variable factors that are regularly reassessed both at the beginning of and throughout the duration of any measurement campaign (both the SMC and the verification campaign)

Section 5.3.2 through Section 5.3.4 below provide a sample of recommended point accuracy considerations and may be incomplete for a particular scanning lidar model as each lidar model varies in design. It is further noted that some factors listed in this paper may not apply to certain lidar models and some factors may be missing for a particular model. Common pointing accuracy tests are included in Appendix B.

5.3.2 System specific factors

Backlash: The backlash effect is described in Appendix B.4. Whether or not backlash is an issue, and the magnitude of the effect, will depend on exact specifications of the specific scanning lidar being used and should therefore be assessed during the verification. Since the backlash can vary a small amount over the lifetime of a scanning lidar, it should be assessed at the start of each pre-campaign verification.

Pointing repeatability: The control system will typically operate using a feedback loop comprised of a motor position and an angular sensor reading. The repeatability with which the scanner will move to a given rotation angle should therefore be assessed during the verification. This is best done by means of a statistical evaluation of several targeting tests with the same reference, and ideally be conducted at different scan rates and for several hard targets to identify possible sensitivities.

Range: The defined range should be compared with the actual distance to the centre of a given range gate. Methods to assess this uncertainty are discussed in Appendix B.6.

5.3.3 Installation specific factors

Inclination sensor alignment: Most lidars have internal pitch and roll sensors. It is recommended that the alignment offset of these sensors relative to the vertical axis of the scanner head be determined after each transport. This is typically done by comparing the sensor values to a series of alignment tests using some form of hard target (such as structures, sea surface, or terrain) and establishing an offset between the two. Methods are described in Appendix B.

5.3.4 Variable factors

Lidar alignment: The pitch, roll, and azimuth orientations (or system frame of reference) will have associated offsets regarding the “global” orientation (global frame of reference) used in determining the relative positions of the lidars to each other and to the measurement points. In an ideal setup, this should only need to be assessed once at the start of each campaign (or each time the lidar is moved). However, some foundations may be subject to settle with time, may bend or move depending on external loads such as wind. How often and with what method to assess the lidar alignment will therefore depend strongly on the installation site. As a rule of thumb, at least one repetition every month is a reasonable requirement and unscheduled repetitions after extreme events (such as a storm or earthquake) are additionally advised.

5.4 LOS wind speed verification

5.4.1 Overview

The aim of the LOS wind speed verification is to determine the measurement accuracy and reliability of the lidar system through a so-called “white box approach.” The current state of the art is to verify the LOS wind speed in the free field against a known reference measurement with well-established uncertainties, typically but not exclusively a cup anemometer mounted on a met mast. The proposed approach is adapted from IEC 61400-50-3, Chapter 7.5 [13].

5.4.2 Methodology

Lidar setup and configuration

To ensure a successful LOS verification, it is recommended that the following points be considered:

Pointing accuracy calibration: The pointing accuracy of the scanning head should be evaluated and corrected for, according to the guidance in Section 5.3. Often, it is convenient to use the anemometer itself as a hard target, to obtain elevation and azimuth offset that can be directly applied at the measurement location (see Appendix B.2 for details of the hard-target calibration method).

Configuration of elevation angle: The lidar's elevation angle should be adjusted to match the height of the reference as closely as reasonably possible without (even partially) blocking the laser beam. This alignment ensures that the lidar measurements correspond to the wind speeds measured at the reference anemometer's height.

Configuring of azimuth angle: It is recommended that the azimuth angle of the lidar system is configured as close as possible to the reference without (even partially) blocking the laser beam. Care should also be taken to avoid the mast and any of its supports or guy wires.

Avoiding backlash impact: As the scanner head might be subjected to the impact of backlash, it is advised to account for it as described in Appendix B.4.

Regular pointing accuracy test: It is recommended to repeat a pointing accuracy test, for example a hard target scan of the reference mast at regular intervals (daily) during the verification period. This practice documents the repeatability of the lidar's pointing accuracy and ensures reliable performance throughout the campaign. See Section 5.3 for guidance on how to do these tests.

Matching measurement settings: The measurement settings (accumulation time and range gate length) during the LOS verification should be consistent to the settings planned for use during the SMC. This alignment ensures comparability of the results.

Data processing and filtering

Using the LOS verification approach, the LOS wind speed (v_{LOS}) measured by the lidar beam is compared to a projected reference wind speed (v_{ref}). The reference wind speed can be determined by using the horizontal wind speed (v_{HWS}) measured by the reference instrument, the beam elevation angle (ϕ), the corresponding wind direction (Θ), and the lidar's azimuth angle (θ) to project the horizontal wind speed onto the LOS (the effect of the vertical wind speed is considered as negligible) see Equation 7:

$$v_{ref} = v_{HWS} \cdot \cos(\phi) \cdot \cos(\Theta - \theta) \quad (7)$$

The projection of the HWS onto the LOS is based on the averaged 10-minute data of the two horizontal wind vectors (*u* and *v* component).

The binning is performed using wind speed bins with a bin-width of 0.5 m/s centred on multiples of 0.5 m/s from 3.75 m/s to 12.25 m/s. In order for the dataset to achieve statistical relevance, this approach requires valid concurrent data from the scanning lidar and reference to meet the following [13]:

- At least 50 hours of valid data (corresponding to 300 10-minute values)
- At least five valid 10-minute data points available within each wind speed bin from 4 to 12 m/s

As the white box approach uses the LOS wind speeds for the comparison analysis, wind conditions up to 16 m/s, as required for profiling lidar verifications, are difficult to achieve during a verification campaign of limited duration. This is because the projected wind speed will always be lower than the scalar wind speed, and so in practice, significantly higher wind speeds would be required to fill the uppermost wind speed bin. For this reason, the IEC 61400-50-3 [13] has set their best practice criterion to 12 m/s. It is noted that even this criterion may be difficult to achieve and therefore a lower threshold that includes wind speeds up to a reasonable estimate of the maximum wind speed to be expected at the SMC site may be set. The data filtering settings should be identical to filtering approach for the observation campaign. Invalid wind sectors (as described in Section 5.2) should be filtered out.

It is recommended that LOS wind speeds from the verification are assessed using a two-variant linear regression:

$$v_{LOS} = a \cdot v_{ref} + b \quad (8)$$

the LOS wind speeds measured by the lidar (y-axis) and the projected reference wind speed measured by the reference measurement systems (x-axis). The regression analysis is performed for both the 10-minute and the binned datasets.

5.4.3 Key performance indicators

Table 5-1 proposes the best practice and minimum key performance indicator (KPI) thresholds that are recommended to be fulfilled for the performance of the lidar to be deemed suitable for use for a wind speed measurement campaign.

Table 5-1 Table of key performance indicators for LOS wind speed verification

KPI	Definition	Acceptance Criteria	
		Best Practice	Minimum
$X_{v_{LOS}}$	**Mean LOS Wind Speed – Slope (a)** Slope of linear regression analysis	0.99 – 1.01	0.98 – 1.02
$OFF_{v_{LOS}}$	**Mean LOS Wind Speed – Offset (b)** Offset of linear regression analysis	±0.1 m/s	±0.2 m/s
$\mathrm{R}^2_{\mathrm{v_{LOS}}}$	**Mean LOS Wind Speed – Coefficient of Determination** Correlation coefficient of linear regression analysis	> 0.99	> 0.98
$C_{v_{LOS}}$	**Mean LOS Wind Speed – Difference** Absolute difference of mean wind speeds between lidar and reference as measured over the whole verification campaign duration, expressed as percentage relative to the campaign mean wind speed.	< 1%	< 1.5%

5.5 Verification of reconstructed wind field quantities

An alternative method to the LOS wind speed verification is to verify the reconstructed wind speed values directly (typically referred to as the black box approach). This approach is used, for example, for the verification of vertical profiling lidars in the IEC 61400-50-2 [16]. The challenge with applying this method to DSL campaigns is to find a test site that enables the scan geometry of the specific measurement campaign to be replicated. Moreover, if multiple locations are planned, then ideally several different scan geometries would need to be verified.

However, this approach is recommended when using a WFR algorithm for the first time, or a non-standard scan pattern (e.g., PPI scans). It can also be beneficial if non-standard device configurations are used, to provide an estimate on how they may influence the final reconstructed wind speed and direction. In this case, the user is advised to consult the IEC 61400-50-2 [16] and apply the method as best as possible to at least one measurement height whilst using the WFR, scanning pattern, and device configuration planned for use in the SMC. The scanning pattern used in the verification should at least recreate the return time and sampling distribution of the SMC.

For a HWS verification, it is recommended that a device should meet the same KPIs that are considered for profiling lidars (see Table 5-2).

Table 5-2 Table of key performance indicators for horizontal wind speed verification

KPI	Definition	Acceptance Criteria	
		Best Practice	Minimum
X_v	**Mean Wind Speed – Slope** Slope returned from single variant regression with the regression analysis constrained to pass through the origin. Analysis shall be applied to wind speed ranges from 4 to 16 m/s given achieved data coverage requirements.	0.98 – 1.02	0.97 – 1.03
R_v^2	**Mean Wind Speed – Coefficient of Determination** Correlation Co-efficient returned from single variant regression. Analysis shall be applied to wind speed ranges from 4 to 16 m/s given achieved data coverage requirements.	> 0.98	> 0.97
C_v	**Mean Wind Speed – Difference** Absolute difference of mean wind speeds between lidar and reference as measured over the whole verification campaign duration, expressed as percentage relative to the campaign mean wind speed. Analysis shall be applied to wind speed ranges from 4 to 16 m/s given achieved data coverage requirements.	< 1%	< 1.5%
X_Θ	**Mean Wind Direction – Slope** Slope returned from a two-variant regression. Analysis shall be applied to all wind speeds above 3 m/s regardless of coverage requirements.	0.98 – 1.02	0.97 – 1.03
OFF_Θ	**Mean Wind Direction – Offset (absolute value)** (same as for R_v^2)	< 5°	< 7.5°
R_Θ^2	**Mean Wind Direction – Coefficient of Determination** (same as for R_v^2)	> 0.97	> 0.95

5.6 Sensitivity to environmental parameters

Given the lack of a defined classification for scanning lidars, it is advisable to closely observe the scanning lidar's response to environmental variables during the verification process. Examples of variables to consider include (but are not limited to):

- Ambient temperature, pressure, and humidity
- HWS (mean and standard deviation)
- Vertical wind speed (mean and standard deviation)
- Wind direction (mean and standard deviation)
- Wind shear
- Wind veer
- CNR

If a notable dependency is identified, it is recommended to add an appropriate additional uncertainty as discussed in Section 7.2.1.2. In general, it is recommended that verification procedures be conducted under climatic conditions as similar as possible to those anticipated for the SMC.

5.7 Post verification

In the event that there are indications that the lidar performance of at least one lidar changed during the course of the campaign, it is recommended to conduct a post-campaign verification along the same lines as the pre-campaign verification to determine if any changes have occurred.

One of the key challenges is how to determine changes in measurement performance during the campaign. This could include installing an independent reference (e.g., a short mast, a vertical profiling lidar) or by comparing the two scanners with each other using some kind of symmetry (e.g., pointing the scanners at 180° azimuth offsets to a point between them). Other alternatives may include a simplified in-situ verification at the start and end of the campaign, with the disadvantage, if a change is identified, of not knowing when during the campaign it occurred. Moreover, the difference of the backscatter value received by both systems at a measurement point can be used as indication of a change in systems performance.

In any case, performing a post-verification is recommended if main components of the systems are changed during the campaign (e.g., laser chain, scanner head) or the firmware has been updated.

5.8 Reporting

At a minimum, reporting should include the following parameters.

5.8.1 General

- Lidar unit: make and model, serial number, year of manufacture, firmware version
- Start and end dates of the verification campaign
- Location / Site(s)

5.8.2 Pointing accuracy

- List of the tested parameters and tests conducted
- Description of the applied methods, especially for azimuth, elevation, and range assessment
- For each reference: Description of reference (e.g., chimney, tower, sea surface, etc.), location, height, bearing, distance, uncertainty associated with location or height, method of determining the location or height of the reference
- Details of other equipment used in the assessment (e.g., theodolite)
- Comparison between pitch and roll offsets obtained from pointing accuracy test to those from the system internal (or added external) pitch and roll sensor(s)
- Results: Azimuth, elevation and range offsets, accuracy, uncertainty, pitch and roll sensor offsets and uncertainty

5.8.3 LOS wind speed calibration

Site and settings

- Site description including terrain, obstacles, free wind direction sectors, pictures
- Description of the reference instruments including make and model, serial number, calibration (date, slope, offset), sketch of met-mast arrangement, method of alignment (for direction sensors)
- Location of lidar and lidar probe volume relative to the reference instrument

- Method of alignment of the LOS
- Lidar settings: range gate length, accumulation time, range gate overlap (range gate separation)
- Time stamp convention (both lidar and reference) and method of synchronisation

Database

- Start and end dates
- Description of lidar quality filters applied to measurement time series
- Description of filters applied to the 10-minute statistics
- Power outages and other significant gaps in the data
- Total number of valid 10-minute data pairs
- Number of valid 10-minute data pairs in each wind speed bin

Results

- Scatter plots of v_{LOS} vs. v_{ref} (10-minute data pairs and bin-wise mean)
- Wind speed linear regression parameters (slope, offset, correlation coefficient)
- Relative mean wind speed difference (for each bin and in total)
- Wind rose for valid data pairs
- One figure with plots of ΔV (1^{st} axis) and $\pm u_{veri}$ (2^{nd} axis) vs. v_{ref} (as in Figure 7 of IEC 61400-50-2 [16])
- Table with calibration results and uncertainties (as in Clause 7.7 of IEC 61400-50-3 [13])
- Deviations from reference in scatter plots and binned by environmental parameters
- Lidar status

6 CAMPAIGN INSTALLATION, OPERATION, AND DATA PROCESSING

6.1 Installation guidelines

6.1.1 System installation

When installing the scanning lidar systems for a DSL campaign, it is advised to follow the manufacturer's guidelines on standard installation of the system and to record the procedure. In addition, there are certain aspects relevant to wind resource assessments with DSLs that may or may not be included in the manufacturer's guidelines but are advised to be considered. These include:

- Installation of a hard, non-deformable surface, if not already existing, upon which the lidar can be installed so that it does not move during the campaign. This is preferably a concrete block or similar.
- A fence around the installation site (ensuring that the beam is not blocked at the measurement positions) or other such systems to prevent access to the system by unauthorised persons or animals.
- If the power supply on site is not sufficiently stable, it is advised that a UPS be installed.

6.1.2 On-site calibration

After installation, it is recommended that the scanner head pointing accuracy be calibrated in accordance with the guidance given in Section 5.3. It is recommended to repeat this process at regular intervals throughout the measurement campaign to determine if the orientation of the device may have changed over time, and to enable corrective action to be taken if needed.

If a suitable wind speed reference exists at (or near) the installation site, a LOS wind speed calibration can be conducted as well, in accordance with the guidance given in Section 5.4 and the IEC 61400-50-3 [13].

6.1.3 Scan configuration

The method with which the scans should be configured will depend on the model of scanning lidar used and the associated software suite with which it is controlled. Furthermore, this document assumes that the scan pattern consists of several individual measurement points, that both scanners point and stare at in a sequential and synchronised manner.

As the time taken to travel between measurement points can differ between the two scanning lidars, it is recommended to ensure that a method is in place to synchronise the measurements from the two systems as closely as possible and within 2s of maximum difference [7]. This could take the form of the quicker lidar waiting for the slower lidar prior to each individual measurement, the lidars resynchronising after each cycle or at regular time intervals (e.g., every full minute).

If backlash has been identified during the verification campaign, then the scans should be set up such that the target elevation is always approached from the same direction.

After the scans are configured, it is advised to check the synchronisation between the lidars and to check that the beam is not blocked at any of the measurement positions.

6.2 Data and system monitoring

During the project it is recommended to frequently monitor several aspects of the lidars' operation, either remotely or on site [17]. This will ensure that the lidars are performing optimally and enable the user to be notified as quickly as possible if any corrective actions are required. Four key types of system parameters must be monitored, as listed below:

- System stability and pointing accuracy: Monitoring the following parameters will help ensure that the position of measurement points will not vary over time.
    - Inclinometer measurements
    - Repeated hard target tests
    - Scanner head status
    - GPS coordinates
- Laser health: System specific laser status parameters should be monitored.
- Lidar synchronization: Monitoring the following parameters will ensure that both lidars' clocks are being well synchronized and that the time synchronization at each point is acceptable.
    - Time synchronization at each measurement point
    - System time synchronization to common server
- System and data availability: Monitoring the following parameters will ensure that the system is monitoring and transferring data reliably. It will also help monitor for any detrimental impact of atmospheric conditions on measurement data availability at the point of interest.
    - Technical availability (past 7 days)
    - Data availability at multiple range gates
    - Remote access status
    - Disk occupation level
    - Internal humidity / relative humidity level

6.3 Maintenance and repair strategy

To ensure maximum system availability throughout the campaign it is important to consider both proactive and reactive strategies for dealing with technical issues that could occur with the scanning lidars.

It is recommended that a routine preventive maintenance program be put in place according to the manufacturer's guidelines to keep the lidar in the best possible working order, increasing their reliability and minimizing the need for reactive intervention [17]. Tasks of this routine maintenance could include, for example, the replacement of desiccants or the cleaning of lidar lenses. It is advised that the frequency and timing of this maintenance be set before the start of the campaign, again according to the manufacturer's guidelines.

For any reactive maintenance or repair, a monitoring system is recommended to provide routine evaluation of system health, notification of malfunction, and any further investigative actions that might be required for the problem to be solved. Such a system should allow for remote monitoring of the lidar and it is recommended that it works continuously with the ability to generate alerts in the case of a serious failure. The recommended monitoring strategy is discussed further in Section 6.2.

It is recommended that an issue escalation plan be defined before the start of the campaign [17] and that reactive maintenance or repair be carried out as soon as practically possible after the failure or malfunction of a component of the dual scanning lidar system. It is advised that most commonly occurring issues with the lidar can be fixed and normal operation restored within 10 working days to minimise the downtime of measurements. In practice this means that the corrective maintenance for these common issues can be performed, remotely or on site, or else that a spare scanning lidar system is available to replace any malfunctioning lidar whilst it is sent for repairs. If a malfunctioning lidar is replaced, it is recommended that the replacement lidar has undergone the same pre-campaign verification process as the original lidar, as detailed in Section 5. If no such pre-verified lidar is available, this may be substituted for a post-campaign verification of the replacement unit. It is also recommended that the installation of the replacement lidar follows the same installation guidelines as the original, as discussed in Section 6.1. Preparations should be made so that resources are available to perform the maintenance and/or swapping of the system in the event of a failure, including the availability of personnel. Any personnel performing the maintenance, repair or replacement of the system should have completed the necessary training for that particular operation according to guidelines set out by the manufacturer.

6.4 Data processing

6.4.1 Data extraction

Continually measuring scanning lidars can generate a large volume of data, which can take a long time to transfer and, in some cases, exceed the inbuilt storage capacity of the lidar computers. A regular data transfer and local backup schedule is therefore recommended to mitigate against data loss.

If the network connection does not allow for high volume data transfers, local data processing for the purpose of monitoring the measurement can be considered. It is recommended to include as a minimum, insight into the pitch and roll angles, internal humidity and temperature values, data availability at each measurement point, the 10-minute averaged wind speed and direction time series, and a webcam or similar image of the device. The more data that can be monitored on a regular basis, the better the ability to identify and address issues that might jeopardise the campaign.

6.4.2 Filtering

Data filters can be applied at multiple stages during the processing, to remove data that are either erroneous or have too much uncertainty. Typically, the first set of filters are applied to the so-called “raw” or “high-frequency” data. The user is advised to refer to the manufacturer’s guidelines for their specific device and that any pre-set quality flags, as well as additional filters on e.g., CNR, are evaluated critically in the context of their particular use case. It is recommended furthermore to consider that the filtering approach used does not affect the measured distribution of wind speed or direction. During the filtering process it is recommended that an unchanged copy of the original measurement data files are kept, to ensure traceability and enable data to be reprocessed, if necessary, at a later stage.

Since the filtering process may reduce the data available for the wind field reconstruction, this can have an impact on the representativeness of the final HWS and direction values at the 10-minute level. A second tier of filters is therefore recommended at the 10-minute statistics level, for example thresholding based on the number of valid samples used to calculate the statistics. While the filters at the raw data level remove data from the subsequent processing steps, it is recommended at the 10-minute level not to remove data, but to flag them according to the quality criteria against which they have been checked. These quality criteria (and the underlying filtering approach) should be documented in sufficient detail to enable users to understand the impact that the filtering process may have on the data quality, and how the inclusion or exclusion of flagged data might impact their further analysis.

6.4.3 Wind field reconstruction and averaging

For the reconstruction of 10-minute averaged measurements, the averaging can either be done on the intermediate quantities (with the averaged values then used to calculate the reconstructed quantities) or on the reconstructed quantities (which are calculated using the instantaneous intermediate quantities for each pair of measurements). Both methods can produce valid results in non-complex flows; however, the choice is not entirely trivial. It is recommended to evaluate the difference between the reconstructed quantities calculated using the two methods. Whichever method is finally used, the choice should be reported. Uncertainties related to this choice are included in the suitability of the WFR to environmental conditions as in Section 7.3.2. If completing a verification of the reconstructed quantities (a “black box” verification, see Section 5.5), it is recommended that the choice of averaging method match that of the reference if applicable.

It is recommended that the WFR be done regularly to allow for regular data transfer and monitoring of the reconstructed parameters.

6.5 Reporting

6.5.1 Installation

- Lidar: manufacturer, model, serial number, date of manufacture, firmware version
- Installation date
- Location: geographic coordinates, height above common datum (e.g., sea level), photographs in all cardinal directions
- On-site calibration (orientation): references (including: name, location, height), method used, offsets (azimuth, pitch, roll), number of measurements, uncertainties
- On-site calibration (LOS wind speed) if relevant: see guidance in Section 5.8.3
- Lidar configuration: range gate length, accumulation time, range gate overlap, measurement positions (azimuth, elevation, range as set in the lidar), scan rates
- Measurement locations: coordinates, height above common datum (e.g., sea level), relative position from lidar (bearing, elevation, range in global frame of reference) scan pattern (e.g., sequence, dwell time, scan rate)
- WFR: type of averaging used, details of WFR, assumptions.

6.5.2 Operation

It is recommended that the monitoring of the parameters listed in Section 6.2, as well as any available environmental data, are routinely documented in a progress report. It is recommended to provide a progress report at least once a week so that unexpected results can be investigated and acted on, mitigating potential interruptions to the measurements.

Furthermore, a logbook should be maintained in which any system changes, errors or deviations in the monitored parameters and corresponding diagnostic activities, power failures or system outages, and repair or maintenance activities are documented.

7 UNCERTAINTY ASSESSMENT

7.1 Overview

The uncertainties of DSL measurements depend on a number of parameters that can vary from project to project. Some parameters are lidar specific while others depend on the individual campaign conditions. Considering the impact of the measurement setup and scan schedule on uncertainty during the design and planning phase can help to reduce the uncertainties significantly by eliminating or minimising some of the parameters through good design.

This section gives guidance on how the uncertainty of DSL wind measurements can be assessed, both pre- and post-campaign. The method for estimating uncertainties described in this section aims to be consistent with that described for nacelle-mounted lidars in Sections 7-9 of the IEC 61400-50-3 [13]. This essentially follows the so-called white box approach, whereby the uncertainty of individual parameters (intermediate quantities) are determined separately and then propagated through the measurement and reconstruction process to arrive at a final uncertainty for the full reconstructed wind speed and direction values.

An alternative, the so-called black box approach, determines the uncertainty for the full reconstructed wind speed and direction values directly through comparison to a reference. This is only touched upon briefly in Section 5.5 which considers the pros and cons of the two methods. However, even when choosing the black box approach, it is useful to understand the individual uncertainty components since the verification and specific measurement campaigns almost always differ to a certain degree, and adjustments to the measurement uncertainty will need to be made.

Detailed documentation of the verification, the setup, and performed pointing accuracy tests are essential to perform a campaign specific uncertainty assessment. Regular repetitions of tests are necessary to describe long-term effects and changes in the setup.

7.2 Uncertainty of intermediate quantities

7.2.1 LOS wind speed uncertainty ($u_{v_{LOS}}$)

7.2.1.1 Determination through verification campaign

The LOS wind speed uncertainty describes the precision achievable by the lidar when measuring the wind speed component parallel to the LOS of the laser. A common way to derive the LOS wind speed uncertainty is using a verification campaign as described in Section 5.4. The LOS wind speed uncertainty can be derived from the verification campaign using the procedure described in clause 7.6 of the IEC 61400-50-3 [13]. The uncertainty of the LOS wind speed comes from the combination of the uncertainty of the reference HWS, the statistical uncertainty of the deviation between reference and LOS wind speeds, and the neglection of vertical wind speed. Figure 7-1 gives an overview of the assessment.

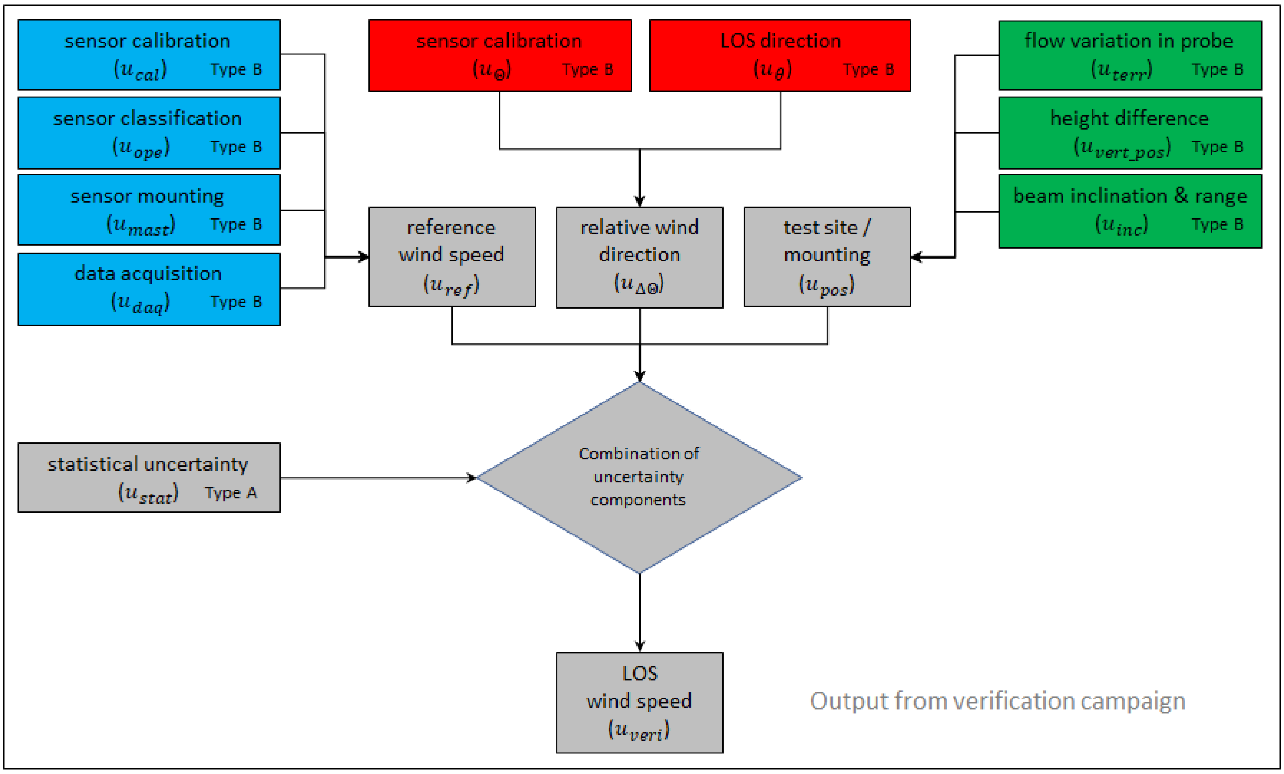

Figure 7-1 Overview of LOS wind speed verification uncertainty assessment ("sensor" in the blue boxes refers to the reference wind speed sensor, in the red boxes it refers to the reference wind direction sensor)

As shown in Figure 7-1 the uncertainty of the reference device (u_{ref}) contributes to the verification uncertainty. State of the art scanning lidar devices can measure the LOS wind speed with an accuracy that is comparable to or even less than that of an IEC compliant cup anemometer. To achieve low verification uncertainty, it is advisable to reduce the uncertainty of the reference as far as possible, by e.g., selecting an anemometer with a high accuracy class or IEC classification number and/or minimising the mounting uncertainty at the reference mast, etc.

In case the SL has a higher accuracy than the reference (e.g., cup anemometer) the resulting verification uncertainty might be conservative. In case the deviation between lidar and reference is larger than the verification uncertainty the reason for that must be investigated and, if justifiable, additional uncertainty should be added.

7.2.1.2 Sensitivity to environmental parameters

The sensitivity of the LOS wind speed uncertainty to environmental parameters should be assessed during the verification campaign as discussed in Section 5.6. If significant dependencies of the LOS wind speed uncertainty to the environmental variables are determined, then additional uncertainties should be applied to the LOS wind speed uncertainty according to the determined relationships. The difference of environmental conditions between the verification and SMC site should be taken into account through interpolation or extrapolation of the determined relationships.

7.2.1.3 Correction for pointing accuracy

In addition to the inherent LOS wind speed estimation uncertainty evaluated during the verification campaign, there are additional uncertainties on the LOS wind speed caused by uncertainties in the azimuth, elevation, and range of the beam. The effect of these pointing angle and range uncertainties can be evaluated at the site of the SMC, taking into account how the variation of measurement height within a wind shear profile can affect the LOS wind speed measurement. The uncertainty of the LOS wind speed due to the propagation of pointing angle and range uncertainties can either be added in quadrature to the corresponding uncertainty obtained through the pre-campaign verification to obtain the corrected LOS wind speed uncertainty or the uncertainty of these variables should be propagated separately through the WFR.

The contributions to the LOS wind speed uncertainty from pointing uncertainties at the site of the SMC can be calculated using shear parameters determined based on the best data available at the site e.g., from flow modelling or nearby measurements in similar conditions. In lieu of suitable data a typical shear can be considered. For a pre-assessment of uncertainty, calculated before the verification campaign has taken place, the LOS wind speed uncertainty to be determined during the verification campaign (u_{veri}) can be estimated based on published verifications using the same model of scanning lidar in similar conditions, or else from the manufacturer's specifications. The contribution to the LOS wind speed uncertainty from pointing uncertainties at the site of the SMC can then be added to this, again being estimated using shear parameters determined using the best available data at the site.

7.2.2 Elevation angle (u_{ϕ})

The elevation angle uncertainty plays a significant role for the overall wind speed uncertainty. Small changes in the elevation angle translate into large changes in the measurement height and thus, depending on the shear profile and the measurement distance, the wind speed measurements.

Therefore, careful pointing accuracy tests need to be performed (the method of which is detailed in Appendix B.2) including estimates of their accuracy. Depending on the method used to calibrate the elevation angle (e.g., hard target, sea surface levelling) the approach to determining the uncertainty will vary. The following list provides some examples of uncertainty contributions to assess:

- Calculation of reference angle
    - If the reference elevation angle is calculated from the known positions of hard targets and the scanning lidar, the relative height of the scanner head to the measurement point and the horizontal distance between them are needed to determine the elevation angle. The uncertainty of these distances can then be converted into an uncertainty of the elevation angle.
- Measurement of reference angles
    - If the pointing accuracy calibration method compares targets with a known elevation angle, seen from the scanner head with a reference angle to that target (as is often the case, for example in hard target calibration), associated uncertainties of the reference angle should be assessed. This reference angle uncertainty can then be converted to an uncertainty of the elevation angle.
- Extrapolation of measured offsets
    - If the measured offset between the reference angle and the reported angle of the beam is extrapolated or interpolated from the reference azimuth and elevation to the azimuth and elevation of the measurement position, as discussed in Appendix B.3, the uncertainty of this extrapolation should be assessed. A Monte Carlo approach can be used whereby artificial errors are applied to the measured angle offsets by randomly sampling a gaussian distribution with standard deviation equal to the standard uncertainty of the reference angle. This process is repeated a significant number of times and the resulting standard deviation of extrapolated angle offsets can be taken as the standard uncertainty of the extrapolation.
    - If the extrapolation uncertainty includes the measurement uncertainty of the reference angles, the measurement uncertainty of the reference angles should be neglected in the final calculation of elevation angle uncertainty to avoid it being double counted.

- If no extrapolation of the reference offsets are necessary (i.e., the reference measurements are taken sufficiently close to the measurement positions), then this uncertainty can be neglected.

- Stability over time
  - Both the stability of the results of the pointing accuracy calibration between successive tests and the long-term stability of the scanning lidar system and its installation over time should be verified and quantified.
  - The repeatability of the pointing accuracy calibration can be assessed by completing several independent tests successively or over a short period of time and studying the spread of their results. In some cases, this may be driven by the angular resolution of the scanning lidar or the reference.
  - Regular repetitions of the initial pointing accuracy calibration over the course of the campaign help to understand the long-term stability, or even indicate the necessity of adjustments during the campaign. The standard uncertainty can be assessed as the standard deviation of the measured elevation offset.

The final uncertainty of the elevation angle is the quadratic sum of all the uncertainty contributions. The procedure for evaluating the elevation angle uncertainty is shown graphically in Figure 7-2.

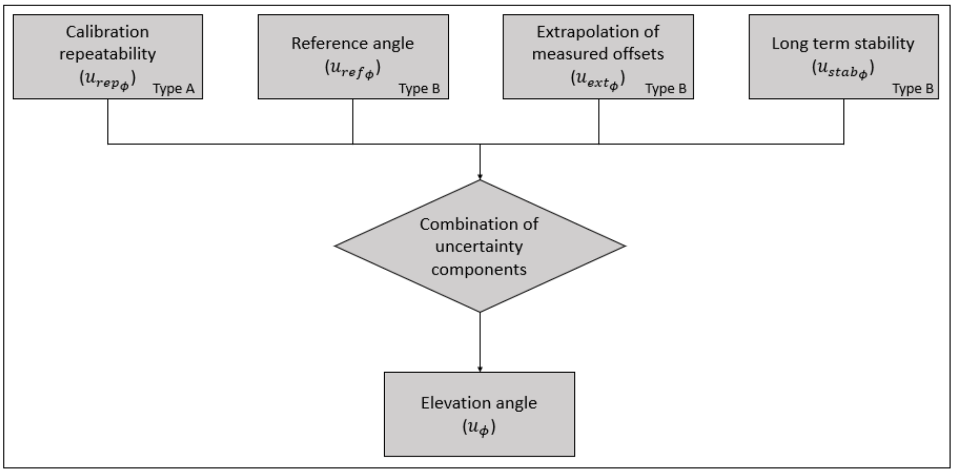

Figure 7-2 Schematic describing the process flow for calculating the elevation angle uncertainty

7.2.3 Azimuth angle (u_θ)

In a horizontally homogeneous atmosphere, the azimuth angle uncertainty has a smaller impact on the uncertainty of final reconstructed quantities than the elevation angle uncertainty, but nonetheless it must be assessed. A similar method to the evaluation of elevation angle uncertainty, as described above in Section 7.2.2, may be employed.

7.2.4 Range (u_R)

The uncertainty of final reconstructed quantities is not very sensitive to the measurement range uncertainty and even a conservative estimate will not have a big impact. Options for the quantification of range uncertainty are discussed in Appendix B.6.

7.3 Uncertainty of the final reconstructed quantities

Once the uncertainties of intermediate quantities used in the WFR have been determined, the final uncertainty of the reconstructed quantities (horizontal wind speed and wind direction are considered in this report) may be determined.

Following the procedure described in the IEC 61400-50-3 [13] the final uncertainty can be calculated from three terms, assumed uncorrelated and therefore added in quadrature:

- Uncertainty resulting from the propagation of the uncertainties of intermediate values through the WFR
- Uncertainty resulting from the suitability of the WFR to the environmental conditions
- Uncertainty resulting from motion of the scanning lidar causing a variation of the measurement location

These are described in more detail in the following subsections. The evaluation of the uncertainty of the reconstructed parameters is illustrated in Figure 7-3, using the HWS as an example.

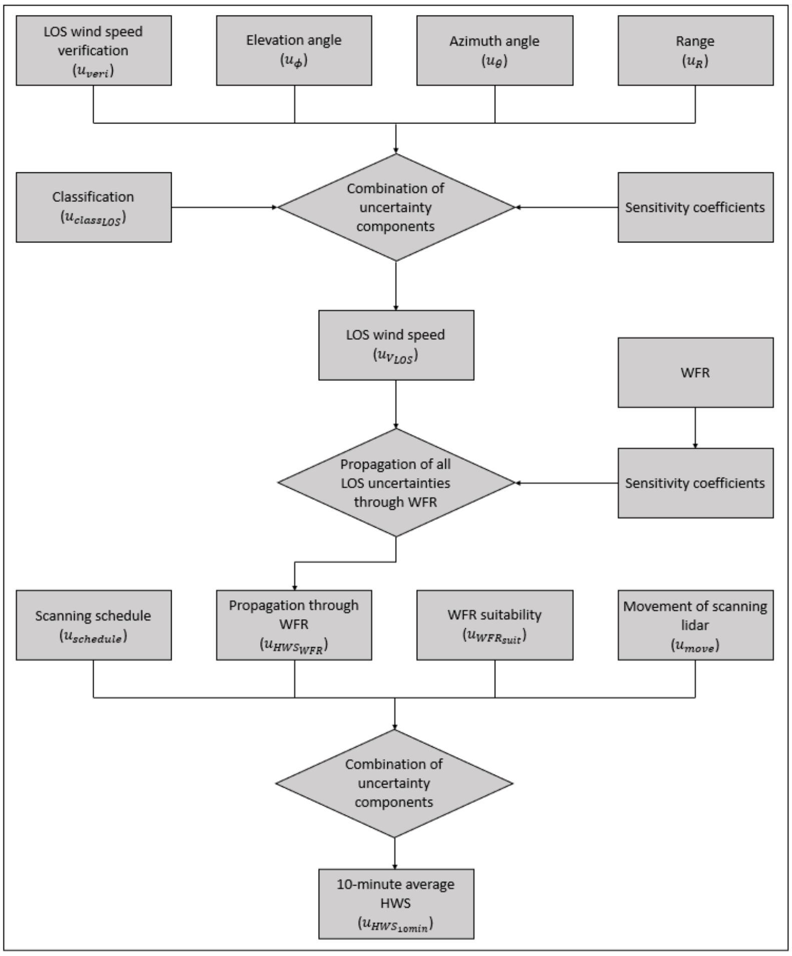

Figure 7-3 Schematic describing the process flow for determining the uncertainty of a single 10-minute average reconstructed HWS

7.3.1 Propagation of uncertainties through wind field reconstruction

If the WFR can be represented analytically in a differential equation, the method described in the GUM [18] for the propagation through a function of the uncertainties of its dependent variables, whilst assuming that they are uncorrelated. This is shown in Equation 9 for some function *f* with parameters x_1, $x_2 \ldots x_k$. An example of this calculation with the WFR equations shown in Equations 5 and 6 is shown in equation A8.

$$u_f^2 = \sum_{i=1}^{K} u_{x_i}^2 \left(\frac{\partial f}{\partial x_i}\right)^2 \tag{9}$$

Note that the effect of azimuth and elevation angles (as well as range) are taken into account in the LOS wind speed uncertainty and so terms containing partial derivatives of these quantities should be neglected here.

If the WFR cannot be represented analytically or differentiated, the uncertainty can be obtained through some other method, such as the Monte Carlo method.

7.3.2 Suitability of the WFR

If the WFR is taking place in conditions where the WFR method has been proven to be suitable through a black box verification according to the guidance given in Section 5.5, this uncertainty can be considered as equal to zero in simple terrain or offshore. If no verification has taken place, or if the SMC takes place in complex flow conditions, an appropriate uncertainty should be added to the final uncertainty of reconstructed parameters to account for this.

7.3.3 Uncertainties due to motion of the scanning lidar system.

If the scanning lidar is installed on a static platform, according to the guidelines in Section 6.1, the variation of measurement location due to movement of the system can be considered as negligible and the resulting uncertainties thus neglected. Note that this is separate from uncertainties of the pointing angles of the beam, inherent to the lidar system, which should be propagated through the WFR as in Section 7.3.1.

If the lidar is installed on a moving platform, such as on the transition piece or nacelle of a wind turbine, then the variation of measurement location due to movement of the system can no longer be neglected. Depending on how the data are treated to mitigate this effect, there are differing recommended approaches to the calculation of uncertainty:

- If the WFR natively takes into account the variation of the measurement location and gives an output at the desired measurement location, the uncertainty of the measurement position can be considered as an uncertainty of an intermediate quantity, as in Section 7.2, and propagated through the WFR as in Section 7.3.1.
- If the variation in measurement location is corrected in post-processing, the method used to do so should be documented. The residual uncertainty of this correction method can be calculated and documented, using the GUM method [18] if applicable.
- If the variation in measurement location is not taken into account or corrected for, either in the WFR or in post-processing, then an uncertainty of the final reconstructed quantities should be calculated. A suitable estimate for these uncertainties is the maximum range of possible corrections, using a conservative shear coefficient, divided by the square root of three as described in the IEC 61400 50-3 [13].

7.4 Reporting

The uncertainty estimation should be described in a transparent and traceable way. This should include:

- List of uncertainty contributors that have been identified / neglected including their values used for assessing the final uncertainty. Containing at least $u_{v_{LOS}}$, u_{ϕ}, u_{θ}, u_R.
- Description and results of quantification methods (statistical / experimental / sensitivity analysis / expert judgement)
- Reference to device classification test, if not available a note on how this was considered.
- Reference to device verification report.

8 REFERENCES

[1] New Energy and Industrial Technology Development Organization, “Offshore Wind Measurement Guidebook” Version 0.1.

[2] Gomez, P., Simon, E. and Courtney, M. “Scanning LiDAR Best Practice for Power Curve Testing,” 2023 rep. Roskilde: Carbon Trust. Available at: https://www.carbontrust.com/our-work-and-impact/guides-reports-and-tools/guidelines-for-scanning-lidars-for-power-curve-testing.

[3] S. Elliot, “Determination of an Optimum Sector Size for Plan Position Indicator Measurements using a Long Range Coherent Scanning Atmospheric Doppler LiDAR,” thesis, 2015

[4] A. Choukulkar *et al.*, “Evaluation of single and multiple Doppler lidar techniques to measure complex flow during the XPIA Field campaign,” *Atmospheric Measurement Techniques*, vol. 10, no. 1, pp. 247–264, 2017. doi:10.5194/amt-10-247-2017

[5] R. P. Davies-Jones, “Dual-Doppler radar coverage area as a function of measurement accuracy and Spatial Resolution,” *Journal of Applied Meteorology*, vol. 18, no. 9, pp. 1229–1233, 1979. doi:10.1175/1520-0450-18.9.1229

[6] R. L’hermite and L. J. Miller, “Doppler radar methodology for the observation of convective storms,” *Radar Meteorology*, pp. 133–138, 1970.

[7] M. Young, A. Oldroyd, M. Shafa, P. Sekar, and P. Schwenk, “Verification of dual-scanning lidar for wind resource assessment: assessing turbulence, long-range and multiple height scanning,” in *Wind Energy Science Conference*, 2023

[8] K. Watanabe, T. Susumu, C. Hemmi, and T. Ishihara, “A study of offshore wind assessment using dual-Doppler scanning lidars,” Journal of Wind Energy, vol. 45, pp. 40–48, Sep. 2021.

[9] S. Shimada et al., “Validation of near-shore wind measurements using a dual scanning light detection and ranging system” *Wind Energy*, vol. 25, no. 9, pp. 1555–1572, 2022. doi:10.1002/we.2757

[10] MEASNET, Evaluation of Site-Specific Wind Conditions, Version 3, 2022

[11] CARBON TRUST, Carbon Trust Offshore Wind Accelerator Roadmap for the Commercial Acceptance of Floating LiDAR Technology, Version 2.0, 2018

[12] Vasiljević, M. Courtney, and A. T. Pedersen, “Uncertainty model for dual-doppler retrievals of wind speed and wind direction,” Atmospheric Measurement Techniques, 2020. doi:10.5194/amt-2020-321

[13] International Electrotechnical Commission: IEC 61400-50-3:2022 ”Wind energy generation systems – Part 50-3: Use of nacelle mounted lidars for wind measurements”, Edition 1.0, 2022-01.

[14] International Electrotechnical Commission: IEC 61400-50-1:2022 ”Wind energy generation systems - Part 50-1: Wind measurement - Application of meteorological mast, nacelle and spinner mounted instruments”, Edition 1.0, 2022-11.

[15] International Electrotechnical Commission: IEC 61400-12-1:2017 ”Wind energy generation systems - Part 12-1: Power performance measurement of electricity producing wind turbines”, Edition 2.0, 2017-03.

[16] International Electrotechnical Commission: IEC 61400-50-2:2022 ”Wind energy generation systems - Part 50-2: Wind measurement - Application of ground-mounted remote sensing technology”, Edition 1.0, 2022-08

[17] World Meteorological Organization (WMO): Manual on the WMO Integrated Global Observing System Annex VIII to the WMO Technical Regulations, Edition 2021. Geneva, 2021. Available at: https://library.wmo.int/idurl/4/55063

[18] Joint Committee for Guides in Metrology, “Evaluation of measurement data – Guide to the expression of uncertainty in measurement, (GUM 1995 with minor corrections)”, 2008. Available at: https://www.bipm.org/utils/common/documents/jcgm/JCGM_100_2008_E.pdf.

[19] V. S. Bagad and G. Subhash, “Mechatronics”, 4th ed. Pune: Technical Publications, 2009.World Meteorological Organization (WMO): Manual on the WMO Integrated Global Observing System Annex VIII to the WMO Technical Regulations, Edition 2021. Geneva, 2021. Available at: https://library.wmo.int/idurl/4/55063

[20] A. Rott, J. Schneemann, F. Theuer, J. J. Trujillo Quintero, and M. Kühn, “Alignment of scanning lidars in offshore wind farms,” Wind Energy Science, vol. 7, no. 1, pp. 283–297, 2022. doi:10.5194/wes-7-283-2022

APPENDIX A UNCERTAINTY CALCULATION – EXAMPLE

This example describes the uncertainty calculation of a wind resource measurement campaign with a dual scanning lidar system.

A.1 Setup

For this example campaign, three virtual met masts have been defined at three near shore locations A, B and C with locations A and C measuring at 140 m above sea level only and location B at 60 m, 140 m, and 220 m above sea level.

Beam intersection angles at each virtual met mast are A: 117°, B: 88°, and C: 63°. Table A-1 gives an overview of the scan geometry. The given angles have been calculated from the lidars to the measurement locations and do not contain any pointing accuracy corrections. These have been considered in the configuration of the devices.

Table A-1 Example scan geometr

	Lidar 1			Lidar 2		
	range [m]	**azimuth [°]**	**elevation [°]**	**range [m]**	**azimuth [°]**	**elevation [°]**
A_140	5715	201.50	1.11	5714	84.84	0.70
B_060	6975	187.37	0.25	6975	98.97	-0.08
B_140	6975	187.37	0.91	6975	98.97	0.58
B_220	6977	187.37	1.57	6976	98.97	1.23
C_140	9363	174.46	0.68	9362	111.88	0.43

A.2 Uncertainty due to wind field reconstruction

In this section, the uncertainties of elevation angel (ϕ), azimuth angle (θ), range (R), LOS wind speed (v_{LOS}), and their propagation through the wind field reconstruction equations are described.

The propagation of these uncertainties is based on an analytical model, also known as YADDUM, described in [12].

As a first step for this example the individual intermediate uncertainty contributors are determined.

A.2.1 Elevation angle uncertainty, u_ϕ

The elevation angle has been calibrated prior to the campaign by a sea surface test using the RHI method. It was completed by hard target tests in different directions to obtain the average offset (as described in B.5.2). The uncertainties of the elevation angle have been determined as described in the table below.

Table A-2 Elevation angle uncertainty contributors

Contributor	Uncertainty value	Comment
Reference angles of hard targets	0.01°	uncertainty of theodolite horizontal alignment and device uncertainty
Repeatability of hard target tests	0.02°	Hard target tests have been repeated (on the same day) and showed slightly deviating results, mainly driven by resolution of the elevation angle of the device (0.01°)
Extrapolation	0.06°	By transferring the sinusoidal curve obtained from the sea surface test to the hard target results some minor deviation remained.
Stability over time	0.07°	Hard target tests have been repeated monthly with slightly changing results
Height of the lidar	0.03°	The uncertainty of the lidar height translates into an uncertainty in measurement height. To account for this, it has been transferred into an elevation angle uncertainty. This is not perfectly correct as only the height but not the angle itself is affected.
Total elevation angle uncertainty, u_ϕ	0.10°	Square root of square sums.

A.2.2 Azimuth angle uncertainty, u_θ

The azimuth has been calibrated by hard target testing. UTM coordinates of the targets have been compared with the observed azimuth angles of the lidar during hard target testing and an offset has been determined.

The uncertainty has been estimated from repeatability, standard deviation of offsets determined by individual hard targets, projection of the UTM grid and long-term stability. A conservative value of 0.5° has been estimated. The azimuth uncertainty does not have a big effect on the overall HWS uncertainty.

A.2.3 Range uncertainty, u_R

The uncertainty of the range has been estimated from a hard target test. The range uncertainty does not have a big effect on the overall HWS uncertainty.

A.2.4 LOS wind speed uncertainty

The uncertainty of the LOS wind speed has been obtained from a verification campaign closely following the IEC 61400-50-3 [13]. The verification result was given as a table binned by wind speed (very similar for both devices), compare Figure A-1.

A linear regression of the binned values has been performed to obtain the slope (relative component) and the offset (absolute component) of the given uncertainties.

BIN lower [m/s]	BIN upper [m/s]	V_{ref} [m/s]	V_{LOS} [m/s]	number of data sets [-] KPI DC2	ΔV [m/s]	σdev, ΔV [m/s]	u_stat [m/s]	u_Vref [m/s]	Ur (k=1) [m/s]	Ur (k=1) [%]
2.75	3.25	3.16	3.19	1	0.03	0.000	0.000	0.067	0.067	2.13
3.25	3.75	3.54	3.55	46	0.01	0.055	0.008	0.055	0.056	1.57
3.75	4.25	4.02	4.02	86	0.00	0.052	0.006	0.061	0.061	1.51
4.25	4.75	4.52	4.50	94	-0.02	0.065	0.007	0.069	0.069	1.53
4.75	5.25	5.02	5.00	128	-0.01	0.058	0.005	0.074	0.075	1.49
5.25	5.75	5.50	5.48	126	-0.02	0.076	0.007	0.080	0.081	1.47
5.75	6.25	5.99	5.96	175	-0.03	0.065	0.005	0.084	0.084	1.40
6.25	6.75	6.52	6.50	227	-0.02	0.070	0.005	0.089	0.089	1.36
6.75	7.25	6.99	6.97	224	-0.02	0.059	0.004	0.093	0.093	1.33
7.25	7.75	7.47	7.45	197	-0.02	0.053	0.004	0.098	0.098	1.31
7.75	8.25	7.98	7.96	115	-0.02	0.068	0.006	0.105	0.105	1.32
8.25	8.75	8.49	8.48	98	-0.01	0.067	0.007	0.110	0.110	1.30
8.75	9.25	9.00	9.00	73	-0.01	0.070	0.008	0.124	0.124	1.38
9.25	9.75	9.46	9.48	69	0.01	0.072	0.009	0.134	0.134	1.41
9.75	10.25	9.97	9.97	54	0.00	0.085	0.012	0.141	0.142	1.42
10.25	10.75	10.47	10.47	34	-0.01	0.080	0.014	0.140	0.141	1.35
10.75	11.25	11.01	11.00	25	-0.01	0.058	0.012	0.149	0.149	1.35
11.25	11.75	11.50	11.49	31	-0.01	0.076	0.014	0.154	0.154	1.34
11.75	12.25	11.88	11.94	11	0.06	0.065	0.020	0.164	0.165	1.39
12.25	12.75	12.53	12.58	10	0.06	0.094	0.030	0.185	0.188	1.50
12.75	13.25	13.01	13.04	7	0.03	0.067	0.025	0.170	0.172	1.32
13.25	13.75	13.45	13.53	6	0.09	0.091	0.037	0.171	0.175	1.30
13.75	14.25	13.83	13.89	3	0.05	0.025	0.014	0.202	0.202	1.46
14.25	14.75	14.64	14.63	1	-0.01	0.000	0.000	0.197	0.197	1.34

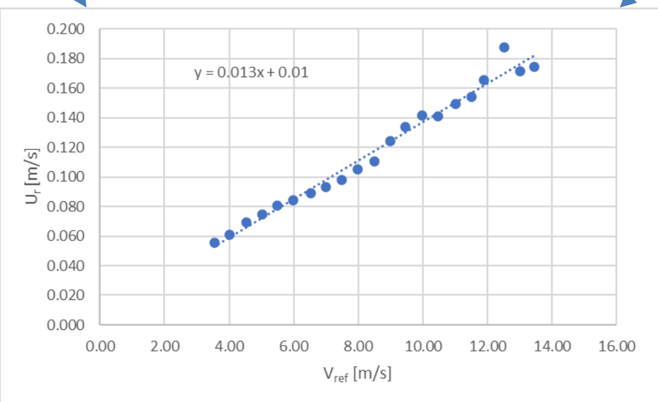

Figure A-1 Example verification results

Typically, a classification uncertainty of the device should be considered, which describes any sensitivities of the LOS wind speed accuracy to environmental parameters. During the verification campaign sensitivities against turbulence, up flow angle, wind shear and veer, air temperature, pressure and CNR have been evaluated. The verification results showed minor sensitivites against turbulence and wind shear with an effect on the LOS wind speed only at overly high values of turbulence and wind shear.

An additional classification uncertainty has still not been considered for following reasons:

- Turbulence and shear values during the offshore campaign are lower than during the onshore verification

- The effect was captured durign the verification campaign and was smaller than the verification uncertainty, therefore it is assumed that the verfication uncertainty [13] is accounting for the observed sensitivites.

It should be noted that no classification of the used scanning lidar has been performed yet. The verification campaign cannot fully replace a classifaction but helps to estimate the effects.

A.2.5 Summary of uncertainty contributors

The uncertainty parameters that go into the calculation of the uncertainty of the reconstructed wind field are summarised in the Table A-3.

Table A-3 Wind field reconstruction uncertainty contributors

Contributor	Uncertainty symbol	Value	Comment
Elevation angle	u_ϕ	0.1°	Includes calibration, repeatability, stability over time, uncertainty of lidar height translated into elevation angle uncertainty.
Azimuth angle	u_θ	0.5°	Includes calibration, uncertainty of reference directions, repeatability, stability over time. Conservative estimate.
Range	u_R	10 m	Conservative estimate determined from hard target test [12].
LOS wind speed	u_{veri}	1.3% of v_{LOS} + 0.01 m/s	From verification uncertainty as per IEC 61400-50-3 [13]
Wind shear coefficient	α	0.15	Conservative offshore value, slightly higher than average measured value

A.2.6 Uncertainty propagation

The uncertainty due to wind field reconstruction depends not only on the scan geometry but also on wind speed and direction. Therefore, individual uncertainty values are calculated for each measured 10-min average of horizontal wind speed and wind direction. In the following, a step-by-step calculation of the horizontal wind speed uncertainty is given. Intermediate results for an example are calculated for better understanding.

HWS and WD values of the example data set at measurement point B_140 are:

v_{HWS} = 7.0 m/s

Θ = 60°

Table A-4 Scan geometry of measurement point B_140

	Lidar 1 (h = 29 m)			Lidar 2 (h = 69 m)		
	range [m]	azimuth [°]	elevation [°]	range [m]	azimuth [°]	elevation [°]
B_140 (h = 140 m)	6975	187.37	0.91	6975	98.97	0.58

Step 1: Calculate line-of-sight wind speeds.

$$v_{LOS} = v_{HWS} \cdot cos(\phi) \cdot \cos(\theta - \Theta) \quad \textbf{(A 1)}$$

Example calculation:

v_{LOS1}= -4.248 m/s

v_{LOS2}= 5.442 m/s

Step 2: Calculate sensitivities for line-of-sight wind speed uncertainties.

Sensitivity of elevation angle uncertainty:

$$\frac{\partial v_{LOS}}{\partial \phi} = -\frac{\alpha}{H_{ref}} Rcos(\theta - \Theta)cos(\phi)^2 v_{H_{ref}} \left(\frac{Rsin(\phi) + (H_l - H_g)}{H_{ref}}\right)^{\alpha-1} + cos(\theta - \Theta)sin(\phi)v_{H_{ref}} \left(\frac{Rsin(\phi) + (H_l - H_g)}{H_{ref}}\right)^{\alpha} \quad \textbf{(A 2)}$$

Please note that in this example H_{ref} can be set to $Rsin(\phi) + (H_l - H_g)$ which results in $\frac{Rsin(\phi)+(H_l-H_g)}{H_{ref}}$ = 1 and $v_{H_{ref}}$= v_{HWS}.

Example calculation:

$\frac{\partial v_{LOS_1}}{\partial \phi_1}$ = 31.68 $\frac{\frac{m}{s}}{rad}$

$\frac{\partial v_{LOS_2}}{\partial \phi_2}$ = -40.71 $\frac{\frac{m}{s}}{rad}$

Sensitivity of azimuth angle uncertainty:

$$\frac{\partial v_{LOS}}{\partial \theta} = sin(\theta - \Theta)cos(\phi)v_{H_{ref}} \left(\frac{Rsin(\phi) + (H_l - H_g)}{H_{ref}}\right)^{\alpha} \quad \textbf{(A 3)}$$

Example calculation:

$\frac{\partial v_{LOS_1}}{\partial \theta_1}$ = 5.563 $\frac{\frac{m}{s}}{rad}$

$\frac{\partial v_{LOS_2}}{\partial \theta_2}$ = 4.400 $\frac{\frac{m}{s}}{rad}$

Sensitivity of range uncertainty:

$$\frac{\partial v_{LOS}}{\partial R} = -\frac{\alpha}{H_{ref}} cos(\theta - \Theta)cos(\phi)\sin(\phi)v_{H_{ref}} \left(\frac{Rsin(\phi) + (H_l - H_g)}{H_{ref}}\right)^{\alpha-1} \quad \textbf{(A 4)}$$

Example calculation:

$\frac{\partial v_{LOS_1}}{\partial R_1}$ = $7.228 \cdot 10^{-5}$ $\frac{\frac{m}{s}}{m}$

$\frac{\partial v_{LOS_2}}{\partial R_2}$ = $-5.916 \cdot 10^{-5}$ $\frac{\frac{m}{s}}{m}$

Step 3: Calculate line-of-sight wind speed uncertainties.

$$u_{v_{LOS}} = \sqrt{u_{veri}^2 + \left(u_\phi \frac{\partial v_{LOS}}{\partial \phi}\right)^2 + \left(u_\theta \frac{\partial v_{LOS}}{\partial \theta}\right)^2 + \left(u_R \frac{\partial v_{LOS}}{\partial R}\right)^2} \quad \textbf{(A 5)}$$

Example calculation:

$u_{v_{LOS_1}}$ = 0.0983 $\frac{m}{s}$

$u_{v_{LOS_2}}$ = 0.1142 $\frac{m}{s}$

Step 4: Calculate sensitivities for horizontal wind speed uncertainty.

Sensitivity of lidar 1 line-of-sight wind speed uncertainty:

$$\frac{\partial HWS}{\partial v_{LOS_1}} = \frac{1}{\sin(\theta_1 - \theta_2)} \frac{v_{LOS_1} - v_{LOS_2}\cos(\theta_1 - \theta_2)}{\sqrt{v_{LOS_1}^2 + v_{LOS_2}^2 - 2v_{LOS_1}v_{LOS_2}\,cos(\theta_1 - \theta_2)}} \quad \textbf{(A 6)}$$

Sensitivity of lidar 2 line-of-sight wind speed uncertainty:

$$\frac{\partial HWS}{\partial v_{LOS_2}} = \frac{1}{\sin(\theta_1 - \theta_2)} \frac{v_{LOS_2} - v_{LOS_1}\cos(\theta_1 - \theta_2)}{\sqrt{v_{LOS_1}^2 + v_{LOS_2}^2 - 2v_{LOS_1}v_{LOS_2}\,cos(\theta_1 - \theta_2)}} \quad \textbf{(A 7)}$$

Example calculation:

$$\frac{\partial HWS}{\partial v_{LOS_1}} = \quad -0.6291 \, \frac{\frac{m}{s}}{\frac{m}{s}}$$

$$\frac{\partial HWS}{\partial v_{LOS_2}} = \quad 0.7951 \, \frac{\frac{m}{s}}{\frac{m}{s}}$$

Step 5: Calculate horizontal wind speed uncertainty due to wind field reconstruction.

$$u_{HWS_{WFR}} = \sqrt{\left(u_{v_{LOS_1}} \frac{\partial HWS}{\partial v_{LOS_1}}\right)^2 + \left(u_{v_{LOS_2}} \frac{\partial HWS}{\partial v_{LOS_2}}\right)^2} \qquad \textbf{(A 8)}$$

Example calculation:

$$u_{HWS_{WFR}} = \quad 0.110 \, \frac{m}{s}$$

Figure A-2 shows the uncertainties due to the wind field reconstruction for all measured data sets of the campaign at the B_140 measurement location (orange), horizontal wind speeds of around 7 m/s are separately indicated (blue) and the value of the example calculation is marked as a cross.

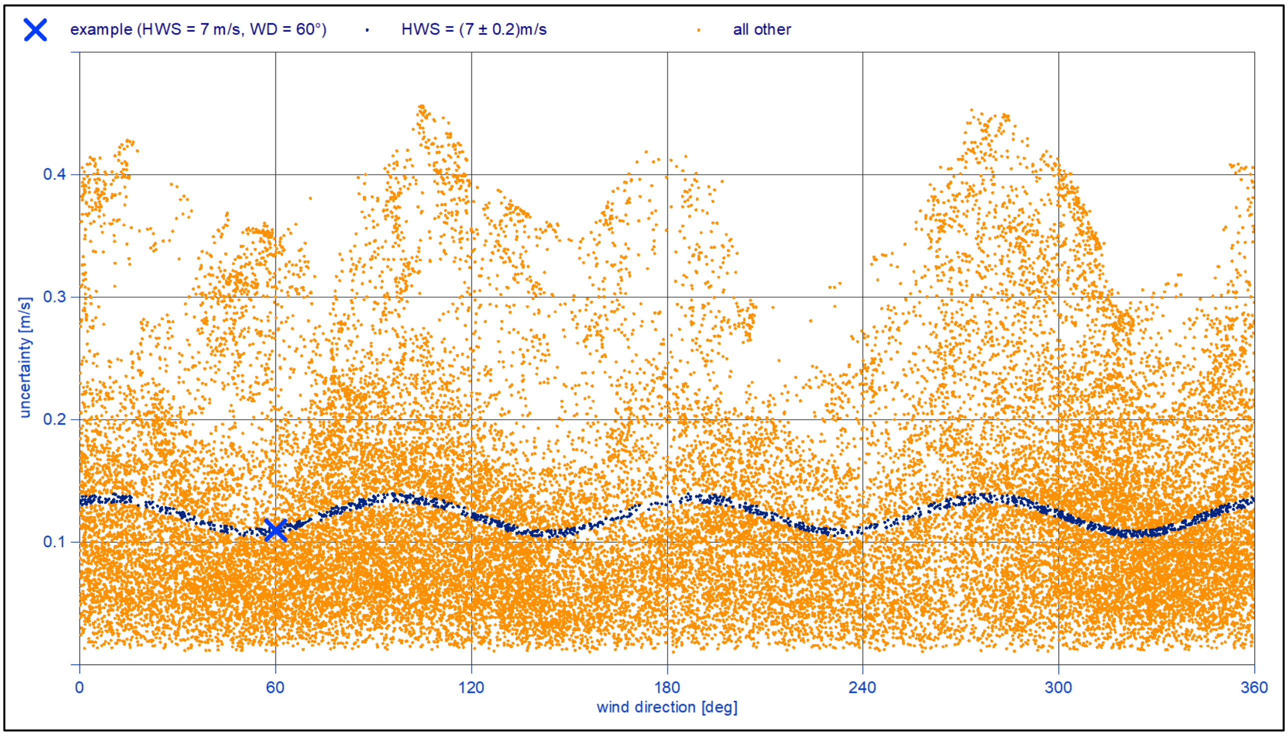

Figure A-2 Example calculation of uncertainties due to wind field reconstruction for measured 10-minute averages of horizontal wind speed as a function of wind direction

A.3 Statistical effect induced by the scanning schedule

The devices have operated in a synchronized manner, measuring each location at the same time with a sampling rate of 1 Hz.

A sequence of measurements (given in Figure A-3) was performed starting at every full minute. Wind field reconstruction has been performed sample by sample (after discarding invalid samples) and horizontal wind speed and wind direction has been stored as 10-minute time series for all locations and heights. Figure A-4 shows an example time series of the measurement location B_140.

total duration 60 sec										
13 sec		7 sec		13 sec		7 sec		13 sec		
measurement B_060	moving time	measurement C_140	moving time	measurement B_140	moving time	measurement A_140	moving time	measurement B_220	moving time	intitialisation

Figure A-3 Example scanning schedule

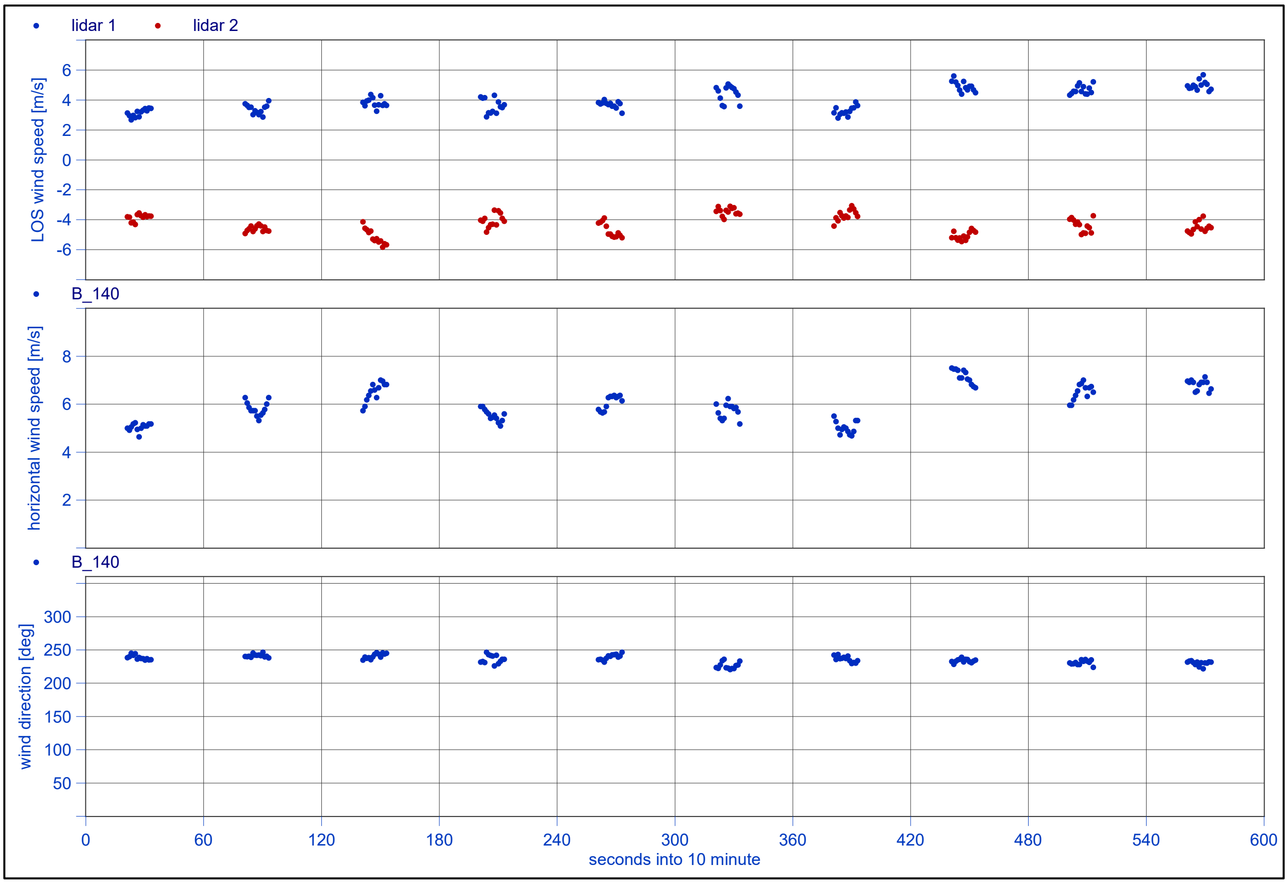

Figure A-4 LOS and reconstructed wind samples within 10 minutes

The effect of measuring only sections of the full 600 seconds induces an additional uncertainty to each 10-minute average.

To evaluate this effect a simulation has been performed based on 1 Hz wind speed measurements recorded at an onshore met mast at a height of 103 m for the duration of one year.

The measured time series have been cut into sections corresponding to the configuration of the lidar. For the example of measurement location B_140 a period of 47 seconds has been discarded after each 13 seconds into the full minute. After discarding the "inactive" periods new 10-minute averages have been determined and compared with the original (full 600 s) averages.

For each 10-min average (simulated and original) the relative wind speed difference has been calculated.

$$diff_{rel,10min} = \frac{WS_{sim} - WS_{org}}{WS_{org}} \tag{A 9}$$

Figure A-5 shows the simulated against the original 10-minute values including a linear regression analysis, the relative differences and their standard deviation binned by the reference wind speed.

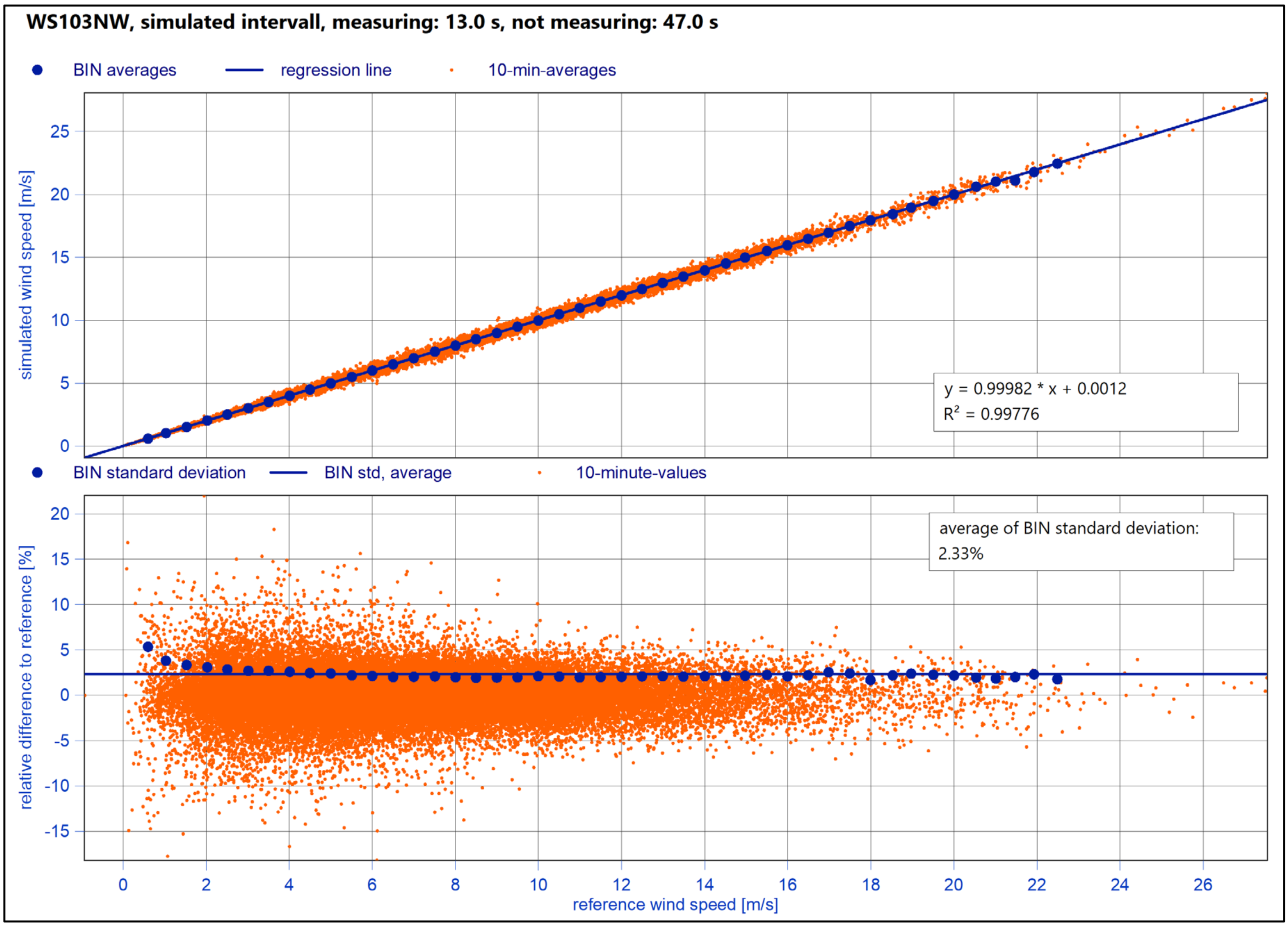

Figure A-5 Simulation of multipoint measurements

Slope and offset of the regression show that no bias is induced into the measurements. If sufficient data are recorded and averaged the result converges to the correct value.

The uncertainty of each induvial 10-minute average can be described by the scatter of the simulated averages around the regression line e.g., standard deviation of the differences.

While the standard deviation of the absolute differences is naturally increasing with higher wind speeds the relative standard deviation remains almost constant for all wind speed ranges and can therefore be better used for further uncertainty evaluations.

For measurement location B_140 all standard deviation bin-values (with each bin containing at least 10 samples) have been averaged to 2.33% which describes the uncertainty of this effect for each individual 10-minute wind speed average.

For the campaign all 10-minute data sets have been used that contain 60 valid samples of data (1 minute) or more. This results in a reduced 10-minute availability for some data sets which is not considered in the simulation described above. Still, it was assumed that the obtained uncertainty covers this effect since after filtering only a few data sets showing an availability below 100%. Also, it could be shown that the uncertainty resulting from such simulations depends on the character of the wind speed time series. For example, the scatter is increasing if the used reference data set is of higher turbulence intensity. It is assumed that the turbulence at the SMC (offshore) location is lower than the turbulence of the reference data set, thus the obtained uncertainty due to this effect is a conservative value.

A.4 Combining the uncertainties

A.4.1 For individual 10-minute averages

The uncertainty of a single 10-minute average of horizontal wind speed can be obtained from:

$$\mathrm{u}_{HWS,10min} = \sqrt{u^2_{HWS_{WFR,10min}} + u^2_{HWS_{stat,10min}}} \qquad \textbf{(A 10)}$$

With $u_{HWS_{WFR}}$: uncertainty due to wind field reconstruction (chapter A.2A.2)

With $u_{HWS_{stat}}$: statistical uncertainty due to multipoint measurements (chapter A.3A.3)

Example calculation:

$$\mathrm{u}_{HWS,10min} = \sqrt{(0.110\,m/s)^2 + \left(0.0233 \cdot 7.0\frac{m}{s}\right)^2} = 0.20\,m/s$$

A.4.2 For averages of 10-minute averages

As the uncertainties of individual 10-minute averages depend on wind speed and direction, it makes it difficult to define a representative uncertainty as an absolute or relative value. Therefore, uncertainties of weekly, monthly, or annual averages have been calculated as follows.

According to the GUM [18] the standard uncertainties u(x) and u(y) propagate into u(z) (with z = f(x,y)) as per the equation below.

$$u^2(z) = \left(\frac{\partial z}{\partial x}\right)^2 u^2(x) + \left(\frac{\partial z}{\partial y}\right)^2 u^2(y) + 2r(x,y)\left(\frac{\partial z}{\partial x}\frac{\partial z}{\partial y}\right)u(x)u(y) \qquad \textbf{(A 11)}$$

With r representing the correlation coefficient of x and y. Simplification can be made for:

r = 0, fully uncorrelated

$$u(z) = \sqrt{\left(\frac{\partial z}{\partial x}\right)^2 u^2(x) + \left(\frac{\partial z}{\partial y}\right)^2 u^2(y)} \quad \textbf{(A 12)}$$

r = 1, fully correlated

$$u(z) = \frac{\partial z}{\partial x} u(x) + \frac{\partial z}{\partial y} \mathrm{u}(y) \quad \textbf{(A 13)}$$

For averaging n wind speed values:

$$avg = \frac{v_{HWS1} + v_{HWS2} + \cdots + v_{HWSn}}{n} \quad \textbf{(A 14)}$$

r = 0, fully uncorrelated:

$$u_{avg} = \sqrt{\left(\frac{\partial avg}{\partial HWS_1} \cdot u_{HWS_1}\right)^2 + \left(\frac{\partial avg}{\partial HWS_2} \cdot u_{HWS_2}\right)^2 + \cdots + \left(\frac{\partial avg}{\partial HWS_n} \cdot u_{HWS_n}\right)^2} \quad \textbf{(A 15)}$$

With $\frac{\partial avg}{\partial HWS_1} = \frac{\partial avg}{\partial HWS_2} = \frac{\partial avg}{\partial HWS_n} = \frac{1}{n}$

$$u_{avg} = \frac{1}{n} \sqrt{u_{HWS_1}^2 + u_{HWS_2}^2 + \cdots + u_{HWS_n}^2} \quad \textbf{(A 16)}$$

r = 1, fully correlated

$$u_{avg} = \frac{\partial avg}{\partial HWS_1} u_{HWS_1} + \frac{\partial avg}{\partial HWS_2} u_{HWS_2} + \cdots + \frac{\partial avg}{\partial HWS_n} u_{HWS_n} \quad \textbf{(A 17)}$$

With $\frac{\partial avg}{\partial HWS_1} = \frac{\partial avg}{\partial HWS_2} = \frac{\partial avg}{\partial HWS_n} = \frac{1}{n}$

$$u_{avg} = \frac{1}{n} \left(u_{HWS_1} + u_{HWS_2} + \cdots + u_{HWS_n}\right) = average\left(u_{HWS_i}\right) \quad \textbf{(A 18)}$$

The uncertainties due to the wind field reconstruction ($u_{HWS,WFR}$A.2) for each individual 10-minute HWS value are considered to be correlated. If an error in one of the uncertainty contributors leads to an over- (or under-) estimation of the wind speed, then it is considered that this over- or (under-) estimation applies for the full duration of the averaging interval (1 month in the current example). This is a conservative approach.

The statistical uncertainties due to scanning schedule ($u_{HWS,stat}$) are considered to be uncorrelated. Wind speed errors induced by this effect are underestimating wind speed at the same level as they are overestimating it.

The final uncertainty of an averaged horizontal wind speed can be obtained from:

$$\mathrm{u}_{HWS,avg} = \sqrt{u_{HWS_{WFR,avg}}^2 + u_{HWS_{stat,avg}}^2} \quad \textbf{(A 19)}$$

With $u_{HWS_{WFR}}$: uncertainty due to wind field reconstruction (chapter A.2)

With $u_{HWS_{stat}}$: statistical uncertainty due to multipoint measurements (chapter A.3)

Table A-5 gives the uncertainties of monthly and overall averages obtained from a 10-month measurements period at B_140. It can be shown that the statistical uncertainties resulting from measuring multiple points can be neglected for this campaign.

Table A-5 Example uncertainties for monthly wind speed averages

Month	HWS [m/s]	n [-]	$u_{HWS_{WFR,avg}}$ [m/s]	$u_{HWS_{stat,avg}}$ [m/s]	$u_{HWS,avg}$ [m/s]
1	8.19	2875	0.1356	0.0042	0.1357
2	7.52	3223	0.1311	0.0039	0.1312
3	8.16	3592	0.1390	0.0038	0.1390
4	7.05	2866	0.1192	0.0035	0.1193
5	6.71	2121	0.1123	0.0039	0.1124
6	7.37	3503	0.1271	0.0036	0.1272
7	7.42	4174	0.1322	0.0031	0.1322
8	6.28	3756	0.1133	0.0028	0.1133
9	6.58	3669	0.1184	0.0031	0.1185
10	9.04	3886	0.1548	0.0040	0.1549
Total	**7.46**	**33,665**	**0.1292**	**0.0011**	**0.1292**

APPENDIX B EXAMPLE METHODS FOR DETERMINING POINTING ACCURACY

B.1 Overview

This appendix looks at methods that can be used to determine the pointing accuracy of the beam of a scanning lidar. These methods are included because they are commonly used. However it is noted that alternative methods both exist currently and could be developed in the future.

The exclusion of such alternative methods from this appendix does not mean that they could not be suitable for DSL campaigns. Any method used to determine the pointing accuracy of scanning lidars used for wind resource assessment should have sufficient proof of its uncertainty and be properly documented.

B.2 Hard target method

Hard targets refer to opaque objects that can be identified by their strong backscatter of the lidar signal when they are hit by the laser, corresponding to a higher CNR than the background. Hard targets can be used in multiple ways to determine different parameters associated with the pointing accuracy, such as azimuth and elevation offset, repeatability of pointing, backlash, or changes in orientation over time to name a few. The hard targets should generally have well defined contours, heights, and positions. Chimneys, turbine towers, or masts are therefore commonly used.

The general principle is to compare the azimuth and elevation angles at which the laser hits these targets to a reference azimuth and elevation angle to obtain azimuth and elevation offsets at particular positions. These reference angles can be measured using, for example, a theodolite or otherwise calculated from the known position and dimensions of the target relative to the scanning head of the lidar.

The above method for determination of azimuth and elevation offsets using hard targets is illustrated schematically in Figure B-1 below. Further examples can be found in IEC 61400-50-3, chapter 7.2 [13].

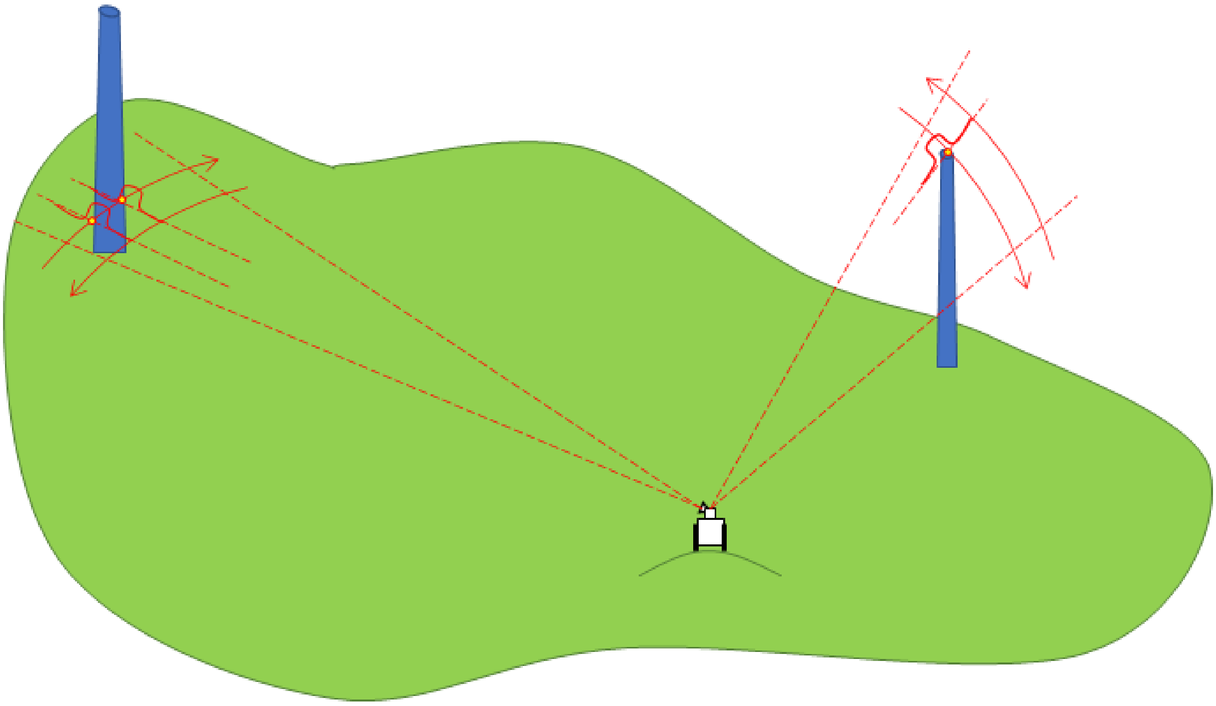

Figure B-1 Schematic showing hard target approach to determine pointing accuracy in azimuth and elevation. Where the beams intersect the target, an increase in the CNR value can be observed, thereby enabling the edges of the hard target to be located in the lidar frame of reference.

It is important to take into account that the offsets in elevation and azimuth are functions of both elevation and azimuth. This means that an offset measured at one elevation and azimuth is not necessarily the same at a different elevation and azimuth. In practice, for DSL campaigns, the elevation angles of the beams are kept low, generally under 5°. If this is the case, the dependency on elevation angle can be neglected and therefore it can be considered that the elevation and azimuth offsets vary only as a function of azimuth.

If the azimuth angle of the reference measurement is close (within 10°) to the azimuth angle of the desired measurement position during the SMC, the reference offset can be considered directly applicable at the measurement position. If this is not the case, the reference offsets should be extrapolated to the measurement positions using the method described below.

B.3 Extrapolation of pointing offset from reference point to measurement position

The scanning lidar beam rotates around axes that are themselves rotated according to the pitch and roll of the system and possibly other factors internal to the scanning lidar device. The implication of this is that offset of the elevation and azimuth angles from the unrotated global frame of reference varies according to a sinusoid function of both azimuth and elevation. Therefore, an offset of elevation or azimuth, measured using a hard target test at one azimuth angle, may not be directly applicable at another azimuth, for example the desired measurement location. Instead, the parameters of the sinusoid should be determined using the results of multiple hard target tests at different azimuths and then the offsets at the measurement location can be interpolated from that curve. Note that all DSL measurements are taken at similar elevation angles (0-5°) the dependence of the offsets on the elevation angle can be neglected.

The relationship between the elevation angle offset and the azimuth angle can be written as in (B 1) and, similarly, the relationship between the azimuth angle offset and the azimuth angle can be written as in (B 2).

$$\Delta\phi = \phi - \phi_{ref} = A_{\phi} \cdot \sin(\phi + P_{\phi}) + O_{\phi} \quad \textbf{(B 1)}$$

$$\Delta\theta = \theta - \theta_{ref} = A_\theta \cdot \sin(\theta + P_\theta) + O_\theta \qquad \textbf{(B 2)}$$

A, P, and O are respectively the amplitude, phase and offset of the sinusoid. To determine these parameters, azimuth and elevation offsets should be measured at (at least) three azimuth angles around the lidar covering at least a sector of 90°. The more offsets that are measured and the more evenly distributed they are around the lidar, the lower the uncertainty of the resulting sinusoid. Two sinusoid curves should be fitted to these measurements (one for the elevation offsets and one for the azimuth offsets). A least-squares minimization is identified as a suitable method to fit the curves, but valid alternatives exist. If an amplitude A_θ of less than 0.5° is expected, a simple average of all the measured offsets or the value taken closest to the measurement point direction can be used. This is due to the low sensitivity of the LOS wind speed uncertainty to the azimuth angle uncertainty and is not recommended for elevation.

Example curves, plotted using measurements from 5 different hard target tests, are shown in Figure B.2.

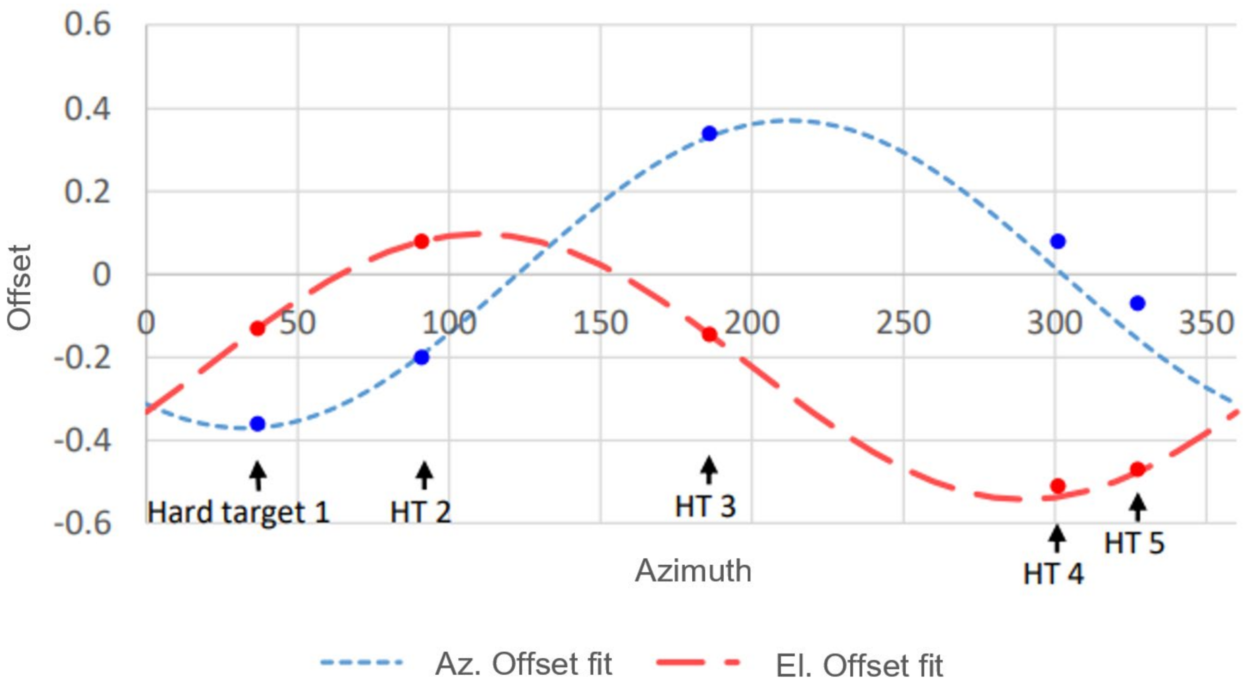

Figure B-2 Directional azimuth and elevation angle offsets

The offsets of azimuth and elevation angle can be interpolated from the determined sinusoids at each of the measurement positions and the scan configurations adjusted accordingly.

This curve now represents the correction which needs to be applied to the theoretical elevation and azimuth angles.

B.4 Backlash

This refers to an effect where motion in a mechanism can be lost when the direction of movement is reversed [19]. This can be caused, for example, by mechanical tolerance in the meshing of gear teeth or the elasticity of belts and can be present in the scanning heads of scanning lidars. In practice, this means that the scanning head can rotate to a slightly different position, depending on whether the requested position is approached from the increasing or decreasing elevation or azimuth angles. Pointing accuracy calibrations can therefore be affected by the direction of motion during the calibration.

The effect of backlash should be considered and if possible quantified during pointing accuracy verification. To quantify the backlash, hard targets should be approached from two directions; for azimuth pointing accuracy, approach the target in the clockwise and anticlockwise directions, for elevation pointing accuracy approach the target from below and from above. Any additional scanning pattern recommendations from the lidar manufacturer should be followed.

B.5 Sea surface levelling

Near a large body of water, the water (or sea) surface can be used as a reference for the horizontal plane. There are multiple approaches to how this can be done. All methods employ a set of downward facing scans and a method for determining the range at which the beam hits the sea surface. Depending on the lidar model used, this may be done using either the CNR values or the LOS wind speeds and a suitable sea entry condition, e.g., drop or rise in signal at the entry point. An example of a method to detect the sea surface strike is presented in [20].

B.5.1 PPI method

One method is to employ a downwards facing circular scan at fixed elevation angle. Plotting the range at which the beam enters the water surface on a polar plot generates an ellipsoid (as shown schematically in Figure B-3) from which the offset of the vertical axis in pitch and roll directions can be calculated. The height of the lidar above the sea surface can also be obtained using this approach.

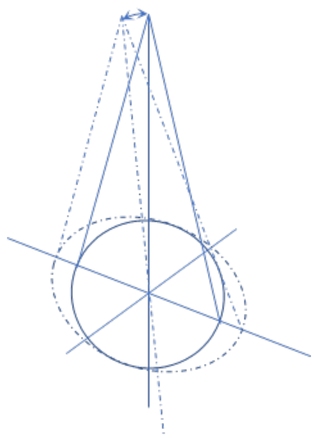

Figure B-3 Schematic representation of the intersect between an inclined surface and conical scan

The determined height of the lidar above the sea surface will be influenced by errors in the lidar range. The vertical angle offset, however, will not be influenced by a fixed range error as this will merely change the size of the ellipsoid but not the length to width ratio.

This method is further elaborated in [20].

B.5.2 RHI method

Another method is to employ several RHI scans at different azimuth angles. For each RHI scan, a fixed range is defined and the elevation angle at which the laser beam at this range is changing from water to air (for increasing elevation angles) or from air to water (for decreasing elevation angles) is determined and recorded.

![DNV logo]

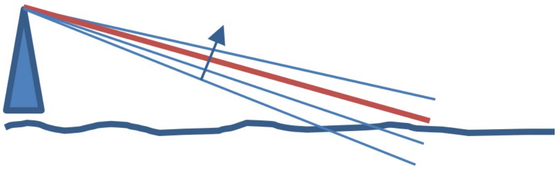

Figure B-4 Sea surface test, RHI method

All detected elevation angles are plotted as a function of the azimuth of the respective RHI scan, and a sinusoidal fit can be applied, similar to the procedure described in section B.3B.3.

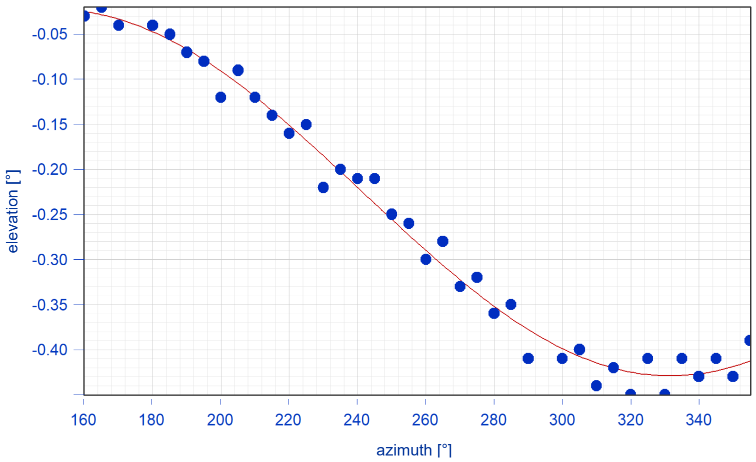

Figure B-5 Sea surface test result, RHI method

The direction which the rotational axis of the device is tilted into is represented by the azimuth angle the curve has its maximum in Figure B-5. This is the same convention as for the curve given in Figure B-1 (multiple hard targets).

That means, the amplitude of the sea surface test can be used as A_ϕ in (B 1) and the phase of the sea surface test can then be used as P_ϕ in (B 1).

The offset of the sea surfaced test cannot directly be used as O_ϕ in (B 1) as it still contains the reference angle defined by height of the scanner head above the sea surface and the specified range for the test (Figure B-6). But it also includes the device specific static elevation angle offset O_ϕ which is the difference of the offset of the curve from the sea surface test and the reference elevation angle ϕ_{ref} .

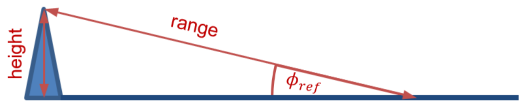

Figure B-6 Reference elevation angle of sea surface test

Knowing the reference angle ϕ_{ref}, O_ϕ can be determined from the offset obtained during the sea surface test $O_{\phi,SST}$ as:

$$O_\phi = O_{\phi,SST} - \phi_{ref} \quad \textbf{(B 3)}$$

The second method is to scan one or more hard targets with known elevation angles. The difference of reference and observed elevation angle is plotted as a function of azimuth angle. The sin curve of the sea surface test is fitted through these values by only changing the offset, amplitude and phase are kept. The offset providing the best fit can be used as O_ϕ in (B 1).

The second method does not rely on the knowledge of the exact scanner head height nor the accuracy of the range.

Good results have been achieved by choosing the range that results in an angle ϕ_{ref} of approximately 0.3° (compare Figure B - 6).

If the available sector for the sea surface test is small, additional hard targets and the measurement points should be in or close to this sector to minimize extrapolation errors.

B.6 Assessment of measurement range uncertainty

The uncertainty of in-the-field calibration methods for the range of lidar measurements is generally higher than the uncertainty of the measurement range itself. However, due to the low sensitivity of the LOS wind speed uncertainty to the measurement range uncertainty (with low elevation beams and in simple flow conditions) even a conservative evaluation is sufficient. It may therefore be quantified using one of the following options:

- Visual observation of the backscatter levels at different ranges, from a target of known position (see the IEC 61400-50-3, Chapter 7.4 [13]).
- Performing a statistical analysis of the LOS speed verification data at different ranges around the reference instrument (see the IEC 61400-50-3, Chapter 7.4 [13])
- Manufacturer’s specifications

About DNV

DNV is the independent expert in risk management and assurance, operating in more than 100 countries. Through its broad experience and deep expertise DNV advances safety and sustainable performance, sets industry benchmarks. and inspires and invents solutions.

Whether assessing a new ship design. optimizing the performance of a wind farm, analysing sensor data from a gas pipeline or certifying a food company's supply chain, DNV enables its customers and their stakeholders to make critical decisions with confidence.

Driven by its purpose, to safeguard life, property and the environment, DNV helps tackle the challenges and global transformations facing its customers and the world today and is a trusted voice for many of the world's most successful and forward-thinking companies.

About Vaisala

Vaisala is a global leader in measurement instruments and intelligence for climate action. We equip our customers with devices and data to improve resource efficiency, drive energy transition, and care for the safety and well-being of people and societies worldwide. With almost 90 years of innovation and expertise, we employ a team of over 2,300 experts committed to taking every measure for the planet. Vaisala series A shares are listed on the Nasdaq Helsinki stock exchange.